THE DESIGN AND PERFORMANCE OF A HIGH EFFICIENCY TRAVELING-WAVE TUBE, THE WJ-274

By Lester A. Roberts

Prepared under Contract No. NAS1-3766 by

WATKINS-JOHNSON COMPANY
Palo Alto, California

for

NATIONAL AERONAUTICS AND SPACE ADMINISTRATION
LANGLEY RESEARCH CENTER

THE DESIGN AND PERFORMANCE OF A HIGH EFFICIENCY TRAVELING-WAVE TUBE, THE WJ-274

By Lester A. Roberts
The Watkins-Johnson Company
Palo Alto, California

SUMMARY

Spacecraft telemetry and communication systems need highly efficient, miniature radio frequency power amplifiers capable of performing during and after launch without degradation due to the severe environments to which they are subjected. This report describes the design approach and the measured performance characteristics of a traveling-wave tube developed for NASA, Langley Research Center designed to meet these requirements. This traveling-wave tube, designated the WJ-274, delivers 20 watts power output over the frequency range 2.2 to 2.3 GHz at an overall efficiency in excess of 36.5 percent. The tube is also capable of operating over the power output range of 10 to 50 watts with good efficiency performance. It requires no modification other than to operate at a different set of voltages and currents. At power output levels of 35 watts and above, the tube exhibits an overall efficiency including heater power of 40 percent. The design basis is described and a wide range of performance characteristics are plotted and discussed.

TABLE OF CONTENTS

	Page No.
INTRODUCTION	1
DESIGN APPROACH	2
PERFORMANCE OF EFFICIENCY, GAIN, AND POWER OUTPUT	10
GENERAL PERFORMANCE OF OTHER CHARACTERISTICS	28
PHYSICAL CONFIGURATION	45
DETAILED SPECIFICATIONS AND ACHIEVED PERFORMANCE (APPENDIX I)	55
TABULATION OF TYPICAL WJ-274 DESIGN PARAMETERS (APPENDIX II)	61

LIST OF ILLUSTRATIONS

Figure No.	Title	Page No.
1	Diagram illustrating the complex interrelationship of tube design factors which control the overall efficiency of a traveling-wave tube	3
2	Normalized phase velocity plot of WJ-274 helix showing band center operating point	5
3	Plot showing relationship of normalized efficiency, η/C, as a function of QC and γb for the slightly overvoltaged case	8
4	Characteristic curves of power output, gain and beam efficiency as a function of helix voltage and beam current	11
5	Characteristic curves of tube nos. 4, 6, 8 and 9 at 50 mA of beam current	13
6	Characteristic curves of tube no. 8 and 9 showing shift in performance by adding only output helix length in tube no. 9	14
7	Smoothed plot of measured data of large signal B, and theoretical curves (Birdsall-Brewer[6]) for small signal B versus over-voltage parameter, b''	17
8	Smoothed plot of experimental data from tube no. 4 showing apparent relationship of beam efficiency to overvoltage parameter	18
9	Plot showing relationship of overall efficiency to beam efficiency and collector depression	20
10	Plot of two stage and single stage collector operation showing no efficiency improvement with the 2nd stage operation	21
11	Current distribution in two stage depressed collector vs collector 2 voltage	22

List of Illustrations (Continued)

Figure No.	Title	Page No.
12	Drawing showing potential gradients and source of secondary electrons which raises helix dissipation and prevents correct two stage operation	24
13	Curves showing single and two stage collector performance	25
14	Broadband power, gain and efficiency characteristics, showing how the power level can be shifted by programming voltages and current without sacrificing gain or efficiency	27
15	Power output vs power input curves at three power levels	29
16	Power output vs power input with maximum efficiency at 2.3 GHz and 35 watts power output	30
17	Power output vs power input with less overvoltaging and lower efficiency than Fig. 16	31
18	Power output vs power input for a tube with additional synchronous helix length ahead of attenuator	32
19	Noise output of tube No. 4 measured in a 1 MHz bandwidth under no drive and saturated drive conditions	34
20	Curves showing noise output and signal output from tube as a function of input power	36
21	Small signal noise figure vs frequency and helix voltage	37
22	Small signal noise figure vs frequency for WJ-274 No. 4	38

List of Illustrations (Continued)

Figure No.	Title	Page No.
23	Plot of AM to PM conversion at saturation vs beam efficiency	40
24	Relative phase shift vs frequency for fixed drive level	42
25	Phase shift and power output vs helix voltage	43
26	Two signal equal amplitude intermodulation product data	44
27	Photograph of the WJ-274 showing a completed tube with magnets in place and a completed body with cathode and header subassemblies to the left and collector subassembly to the right	46
28	Photograph showing the WJ-274 body subassembly and its component parts including strip transmission line and vacuum window	47
29	Photograph of the electron gun and input stripline subassembly and component parts	49
30	Photograph of the collector subassembly and its component parts	50
31	Photograph of the encapsulated WJ-274 No. 4	52
32	Photograph of a lighter weight version of the WJ-274 capsule	53
33	Photograph of another version of the rectangular capsule using mounting feet with access from above and OSM connectors	54

INTRODUCTION

This program was undertaken by Watkins-Johnson Company for the NASA Langley Research Center with the primary objective of developing a small lightweight traveling-wave tube with a very high dc to RF conversion efficiency. The intended use of the tube is for space-craft communications and telemetry systems and therefore special environmental and life requirements are also specified. The tube must perform overwide temperature ranges, under large shock, random vibration, large static acceleration and sea level to space vacuum environment. The design also must include long life capability and high reliability.

A detailed listing of the specifications of the tube is given in Appendix I. The principal requirements and performance of power, efficiency, and gain will be reviewed here.

Power Output

The power output requirement is 20 watts. This is easily obtained and the tube exhibits almost no fading at this power level. The fading referred to here is that caused by heating of the helix and is observed as a decrease in saturation power output as a function of time in the period immediately following application of RF drive to the tube. Typical fading varied from no perceptible fading to a maximum of 0.1 dB from tube to tube.

Saturation power output of the tube was found to be variable over the range of 10 to greater than 50 watts through choice of beam current and helix voltage. The choice of the correct combination of these two parameters could lead to optimum efficiency conditions at any power level.

Efficiency

The overall efficiency requirement including heater power is 40 percent. This efficiency was achieved at the 35 watt level and above. The best efficiency that was achieved at the 20 watt level was 36.6 percent. In general, efficiency increases with the saturation power level of the tube. At the 10 watt level, an overall efficiency of 33 percent was realized. This increased to 40 percent at power levels above 35 watts.

Gain

The saturation gain requirement is 30 dB. Saturation gain values between 20 to 36 dB were achieved on various tubes depending upon the particular design. Because of the large overvoltage condition under which the tubes were operated, it was found that gain

was difficult to predict accurately. However, by making a composite design where the section of the helix ahead of the attenuator operates at maximum small signal gain and the section following the attenuator under the overvoltage conditions, gains in excess of 30 dB could be easily achieved without excessive tube length.

DESIGN APPROACH

The factors which control the over-all efficiency of a traveling-wave tube have a very complex interrelationship and the choice of the proper combination of these factors is important to achieve the optimum performance. A diagram illustrating the qualitative relationship of these factors is shown in Fig. 1.

In general, the larger any of the factors in the bottom horizontal row, the larger will be the overall efficiency. There are certain restrictions on the values of QC and γb based upon previous experimental work and large-signal digital computer studies. There are also limitations on beam perveance set by the ability to focus the electron beam under saturated conditions. The achievable peak magnetic fields and magnet period are in turn limited by the properties of permanent magnet materials.

During the course of the development program, our ideas of the relative importance of the various factors were modified by the experimental results. In general it was found that higher beam efficiencies could be achieved than was expected, that overvoltage operation played a more important role than anticipated and that lower beam perveance had to be used because of limitations imposed by beam defocusing and reflected electrons from the collector.

Helix Design

It is important to have as high an interaction impedance of the helix as possible so that the design value of the gain parameter, C, can be achieved with as low a beam admittance, I_o/V_o, as possible. The lower the value of beam admittance, the easier the focusing problem becomes.

The higher interaction impedance is achieved by using a band center γa of 0.95 and a dielectric loading factor (DLF) of .79. This DLF is obtained by using beryllium oxide wedges for the helix support. This has a two-fold advantage. The lower dielectric constant of the beryllia ceramic compared to the higher value of the more commonly used alumina ceramic leads to a considerable improvement in the DLF. It also performs an excellent job in cooling the helix by its high thermal conductivity. The wedge shaped support rods further reduce the amount of high dielectric material in close proximity to

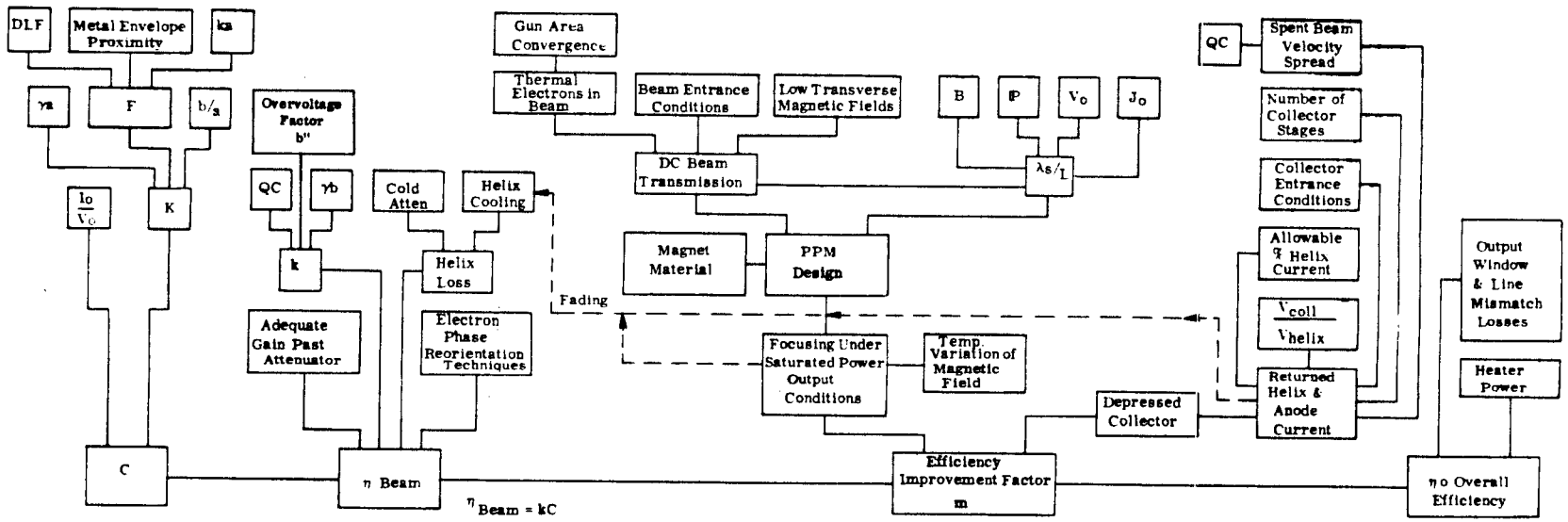

$K = F \cdot f(\gamma a, b/a)$

$C = \left(\frac{I}{V_o}\,\frac{K}{4}\right)^{1/3}$

DLF = Dielectric Loading Factor
ka = $\frac{2\pi a}{\lambda_o}$
a = Mean Helix Radius
λ_o = Free Space Wavelength
γa = $\frac{2\pi a}{\lambda g}$
λ_g = Guide Wavelength
b = Beam Radius
F = Impedance Reduction Factor

C = Gain Parameter
I_o = Beam Current
V_o = Beam Voltage
K = Interaction Impedance
η_{Beam} = Beam Efficiency
k = Efficiency Factor (η/e)
γb = $\frac{2\pi b}{\lambda g}$
QC = Space Charge Parameter
P = Beam Perveance

J_o = Beam Current Density
λ_s = Beam Scallop Wavelength
L = Magnet Period
η_o = Over-all Efficiency
m = Efficiency Improvement Factor of the Collector
B = Rms value of magnetic field
b" = Overvoltage velocity parameter

Fig. 1 - Diagram illustrating the complex interrelationship of tube design factors which control the overall efficiency of a traveling-wave tube.

the helix and thus also helps to improve the DLF. A normalized phase velocity plot of the helix is shown in Fig. 2.

The interaction impedance could be raised further by going to an even lower bandcenter γa helix design. This, however, makes the focusing of the electron beam more difficult. The helix becomes smaller in diameter which in turn forces the beam to be smaller and raises the current density. The magnetic field requirements may then become impractical. Wall loading effects also become large at low γa. The bandcenter γa of 0.95 has been found to be a good compromise.

Cooling

There are three sources of helix heating in a tube design such as this. They are

1. RF losses in the output section

2. Primary interception due to beam defocusing caused by velocity spread and beam expansion under saturated output conditions and

3. Reflected electrons from the collector caused by the depressed collector operation for efficiency improvement.

It is very important in a high efficiency tube to drain this dissipated heat out from the helix so that the helix does not rise to excessive temperatures. Heating raises both the skin effect loss of the helix as well as dielectric loss of the helix support and leads to fading and loss of efficiency. The beryllium oxide support of the helix, because of its high thermal conductivity, leads to a lower temperature difference from the inside surface of the wedge which is in contact with the helix to the outside surface which is in contact with the body wall of the tube. It is also just as important for a good thermal transfer of the heat from the back of the wedge to the body wall. This can be accomplished by an accurate fit between helix and body with the addition of a large net pressure by the wall on the back of the wedge. There also needs to be adequate surface area over which the heat transfer can take place. This is accomplished in the WJ-274 by matching the radius of curvature of the back of the wedge to that of the barrel.

The heat drain from the outside of the body is accomplished through the combination of the magnet pole pieces which are brazed onto the body and the magnets themselves. This heat is then conducted into the heat sink through the capsule of the tube. Each interface between materials must be considered to make sure that operation of the tube in a vacuum environment will not introduce a heat transfer problem. All gaps must be filled with potting materials.

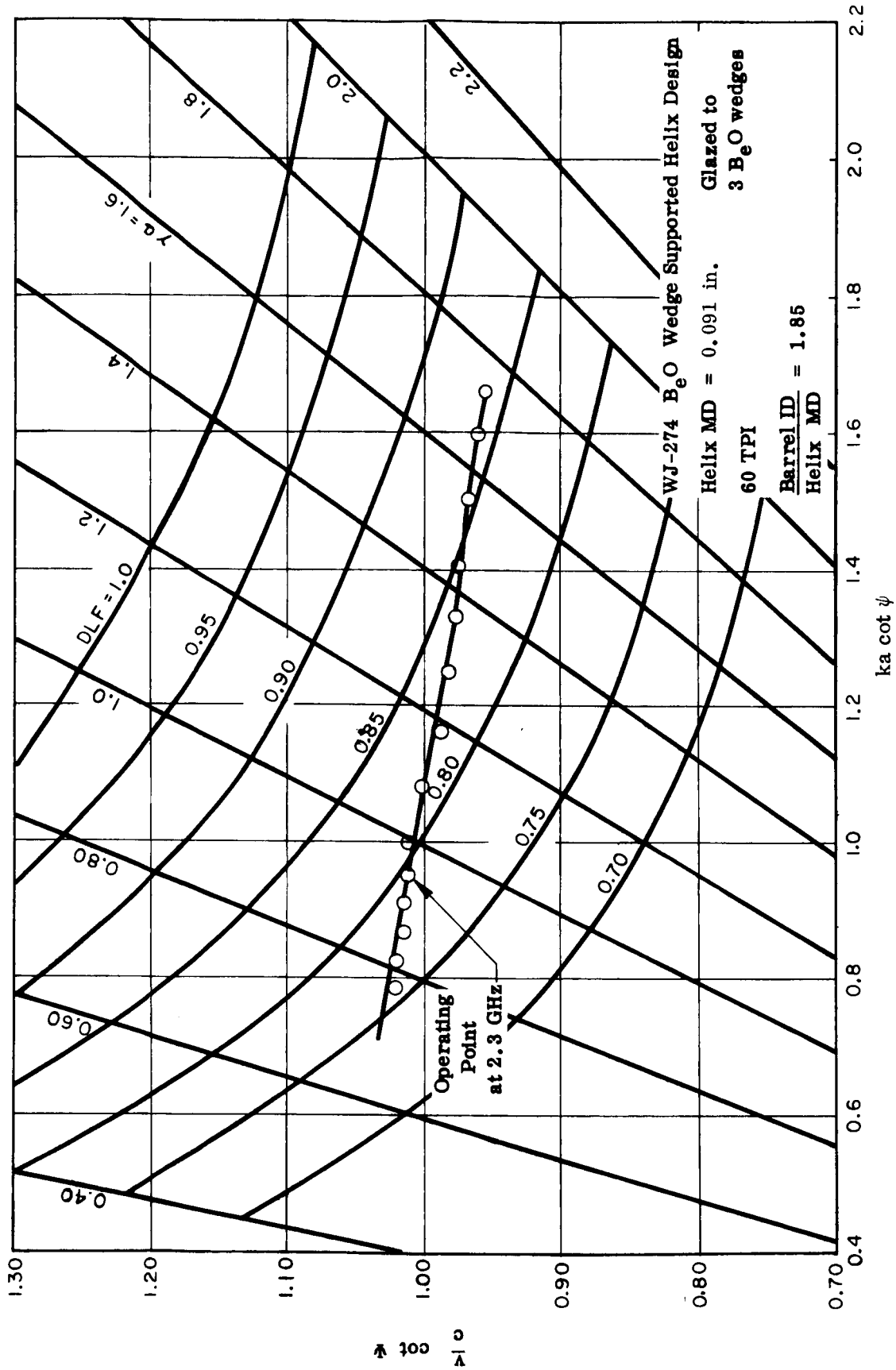

Fig. 2 - Normalized phase velocity plot of WJ-274 helix showing band center operating point.

Large Overvoltage Operation

The term "overvoltage" as used here is defined to mean the excess voltage applied to the helix above that which corresponds to maximum small signal gain. The precise way of defining it mathematically is in terms of the velocity parameter, b, which will be covered in detail in a later section.

It has long been known that applying an overvoltage to the helix under large signal conditions will increase its power output and also in general increase the beam efficiency as well. In a typical tube design, an overvoltage of 10 to 15 percent is not uncommon for improvement in the saturated power output of a tube. In an octave bandwidth tube overvoltage often cannot be used at all because of its drastic effect upon the gain performance at the high frequency end of the band due to dispersion of the helix phase velocity. But in situations where the requirement is narrowband, such as in most space communication applications, optimizing performance by overvoltage is allowable. The drawback of overvoltage operation is that both the small signal and saturation gain of the tube is reduced. In a typical case, as the helix voltage is increased, the saturated power output will rise, reach a maximum and then fall for any further increase of voltage. As voltage is increased, the tube gain decreases and the RF drive signal must be increased to drive the tube to saturation. The factor that limits the maximum improvement in power output and thus the efficiency is not an excessive overvoltage, but the fact that the gain beyond the attenuator has decreased to the point where maximum efficiency can no longer be achieved. This has been shown by Scott[1] and others to be about 26 dB of small gain beyond the attenuator.

From this line of reasoning it follows that in order to take advantage of larger overvoltage effects and perhaps a further improvement in efficiency, it is necessary to increase the length of helix beyond the attenuator. This increases the gain in this section and allows a larger overvoltage ratio to be applied before the gain limitation begins.

This idea has been successfully applied to the WJ-274 and it currently operates at approximately 1.5 times the voltage that gives maximum small signal gain. The gain of the tube at small signal synchronous voltage is approximately 70 dB and most of this is located after the attenuator. As a result, beam efficiency improvement by more than a factor of two has been achieved under the overvoltage conditions and net gain of the tube in the 20 to 30 dB range is achieved.

QC and γb

The design values for QC, the space charge parameter, and γb, the normalized beam radius, were chosen from earlier experimental work by Cutler[2] which has been confirmed by large signal computations by Tien[3] and Rowe[4]. This work indicated that optimum efficiency would be obtained for values in the region of QC = 0.15 to 0.25 and γb = 0.4 to 0.6 . This is shown in a reproduction of Cutler's plot for slightly overvoltaged conditions in Fig. 3.

It may be that these values of QC and γb are not optimum for the large overvoltage case, but the values were chosen as a basis to begin the design.

Depressed Collector Operation

Depressed collector operation is used to recover as much of the unused dc beam power as possible and thus improve overall efficiency by reducing the power input to the tube. Provisions are made to have two collector stages that can be operated at independent potentials. The actual construction of the collector allows for the cooling of the electrodes to take place by conduction to the tube capsule while simultaneously allowing the voltages to be insulated from ground.

The main precaution in the design of the collector entrance was to make sure that the entering electrons did not strike the lip or entrance tunnel to the collector. In this way there would be no secondary electrons formed in a region where the electric field gradient between the helix and the collector would draw them back into the helix. Thus the emerging electrons from the collector as it is depressed represent true secondaries and reflected primaries from the interior region.

Cathode Design

Two factors govern the choice of the cathode design. These lead to conflicting requirements. Since the power to heat the cathode is included in the overall efficiency calculation, it is desirable to keep the heater power necessary to bring the cathode to the operating temperature to an absolute minimum. One of the major factors in cathode power loss is the heat radiated from the cathode surface. This power loss is proportional to the cathode surface area. Thus it is desirable to minimize this which means the cathode diameter should be kept as small as possible. Life requirements on the other hand would dictate a low current density which dictates that the cathode emitting surface should have as large a diameter as possible. A compromise has been chosen at a cathode current density of 200 mA per cm^2. This

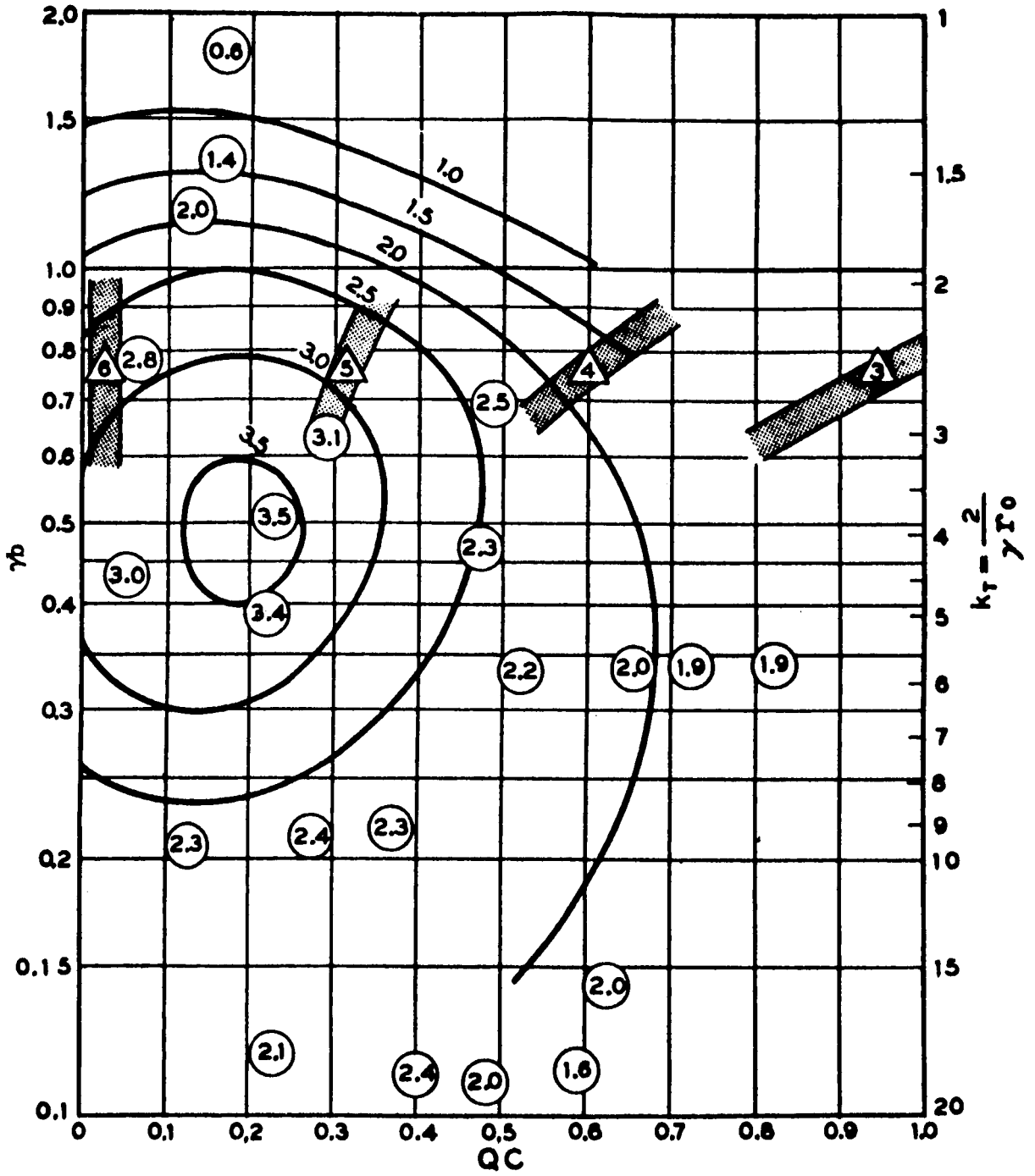

Fig. 3 - Plot showing relationship of normalized efficiency, η/C, as a function of QC and γb for the slightly overvoltaged case. Circled numbers are measured values of η/C from Cutler[2].

1198A

current density allows a cathode operating temperature of 720° C at which temperature an operating life of 50,000 hours can be predicted.

For extreme long life tubes, the end of life must be determined by the depletion of the electron emitting materials of the cathode. This means that depletion of the barium oxide cathode coating by conversion into barium must be the determining factor. The depletion time is determined by certain physical and chemical factors of the cathode and the coating. The coating can be damaged, however, by bombardment of positive ions generated in the electron beam and which are accelerated into the cathode surface. For the coating depletion time to be determined by its chemical reaction rates, the cathode must be protected from this ion bombardment. This is accomplished by designing the electron gun to have an anode voltage at least 50 volts positive with respect to the helix at the operating cathode current. This is a standard procedure on most tubes of this type. It does not pay to make the final gun design until the final operating beam current and helix voltage have been determined and this cannot be done until all the other electrical requirements have been met by the design.

Choice of Beam Perveance

Beam perveance was chosen to have as large a value as possible consistent with the ability to obtain a well focused beam under saturated RF conditions. This then leads to high gain per unit length and leads to the shortest length for a given gain requirement. As the perveance is pushed towards higher values, in the limit it requires that the highest coercive force permanent magnet material be used. The parameter which must be considered from the beam defocusing standpoint is the ratio of beam scalloping wavelength to magnet period, λ_s/L. The scalloping wavelength which must be considered is that of the electrons which have been slowed down the most by the RF interaction. These are the electrons which will be intercepted on the helix as the beam goes into saturation. As they slow down, they begin to approach the periodic-focusing stopband velocity and are lost from the beam onto the helix.

As the tube is made more efficient, more slow electrons are developed in the beam and an appreciable number will have a shorter scalloping wavelength. To keep these electrons from being lost from the beam onto the helix, the magnet period must be made shorter. To maintain a given peak magnetic field in each magnet cell as the period is made shorter requires either larger diameter magnets or higher coercive force material or both.

Initial paper designs were chosen for a beam perveance of 1.5×10^{-6} but it was soon realized that the beam defocusing under RF saturation conditions would be intolerable. Maximum perveance was then chosen to be 1.2×10^{-6} and typical operation occurs in the range from 0.75×10^{-6} and up.

PERFORMANCE OF EFFICIENCY, GAIN, AND POWER OUTPUT

In this section of the report, the performance of various WJ-274 designs is plotted to show the relationship which has been measured between the basic performance characteristics (i.e., efficiency, gain and power output) and the operating voltages and currents of the tubes. Various tube designs were built and tested in an attempt to empirically determine the relationship between the tube design parameters (helix phase velocity, C, QC, beam current, helix voltage, etc.) and performance. This relationship is not yet rigorously understood, but general guide lines for the design have been determined. Many performance curves are plotted in this section to show some of the general forms of variation that can be expected. The curves which are shown are only a sampling of the data that exists.

Also in this section, the idea that the velocity parameter, b, is actually a composite of two other velocity parameters is introduced. The velocity parameter, b, breaks into two components b' and b''. b' is a function of QC and C, while b'' is a measure of the overvoltage conditions under which the tube is operating. It is shown that there is a theoretical basis for choosing b'' based upon small signal parameters which control gain and that there appears to be a relationship between b'' and efficiency.

Power Output, Efficiency and Gain Relationships in an Overvoltaged Tube

Figure 4 shows the relationship typically seen between the operating parameters, helix voltage and beam current, and the performance characteristics of saturated power output, gain and beam efficiency. These curves show the enhancement of beam efficiency resulting from large overvoltage conditions. Here the beam efficiency has risen to 33 percent at the highest beam current level. It should be emphasized that the efficiency shown is beam efficiency not the overall efficiency of the tube which includes the effect of depressed collector operation. Efficiency improvement beyond that shown can be achieved by using collector depression. However, it should be kept in mind that Fig. 4 and following curves are plotted to show the beam interaction effects.

In general, as would be expected, saturated power output increases with increasing helix voltage and beam current. At a fixed value of beam current, the efficiency rises to a maximum as helix voltage is increased and then rapidly falls for a further voltage increase. At the same value of beam current, the saturated gain linearly falls with increasing helix voltage while the power output rises until the efficiency maximum is reached. It is interesting to note at the efficiency maximum that the

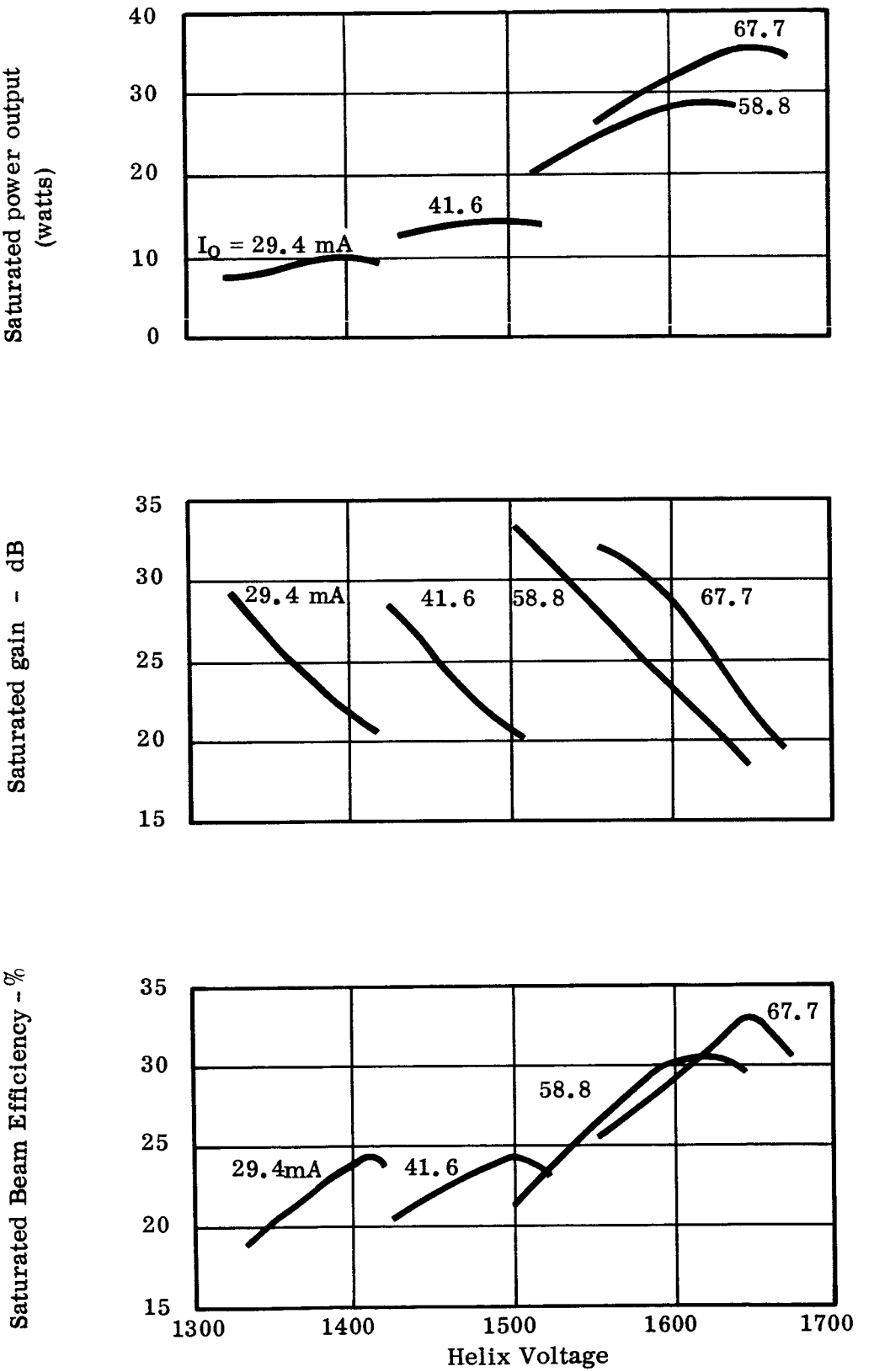

Fig. 4 - Characteristic curves of power output, gain and beam efficiency as a function of helix voltage and beam current. WJ-274 No. 4.

saturated gain has always decreased to 21 dB. Under these conditions, calculations show that practically all of the gain is located in the section of helix beyond the attenuator. Allowing for a 6 dB beam coupling loss through the attenuator, the total electronic gain beyond the attenuator is then 21 + 6 or 27 dB which corresponds closely to Scott's results[1] for minimum required gain beyond the attenuator for maximum efficiency.

In Figure 4, it is seen that for currents above 42 mA and helix voltage above 1500 volts, beam efficiency takes a rapid increase. This occurs in the range where the small signal gain is 0 to 10 dB. Analysis shows that the overvoltage velocity parameter, b'', has a value in excess of about 1.5. Under these conditions, there is very little gain along the length of the helix except in approximately the last inch.

During the course of the development, changes were made in the helix design to increase the beam efficiency without raising the power output. These are summarized in the results plotted in Fig. 5 for all tubes operating at the same beam current. This shows four different tubes with successive changes in the helix design. Tube No. 6 has an increased TPI of both the input and output helix over that of Tube No. 4. The helix voltage for maximum efficiency decreased to 1510 volts. This change did not improve efficiency, in fact, efficiency decreased slightly. Tube No. 8 has a further increase in TPI in the output helix which brought the voltage for maximum efficiency down to 1350 volts and increased efficiency slightly over that of tube no. 4. No. 8 has one other significant feature. The input helix is a different TPI than the output section. It is designed to operate near small signal synchronous voltage in the input section thereby increasing the overall gain of the tube. This did indeed work, and the gain at maximum efficiency is 31 dB. Tube No. 9 has the same helix TPI in the input and output sections and differs from No. 8 only in that the output section of the helix is approximately 1 inch longer. This had the effect of lowering the helix voltage for maximum efficiency even further, but beam efficiency did increase to over 30.5 percent. Simultaneously the gain at maximum efficiency increased to 35 dB.

Figure 6 shows a comparison of the operating characteristics of tubes no. 8 and 9 over a range of beam current values. It shows that there is considerable improvement in the beam efficiency of tube no. 9. Also the maximum efficiency values at different currents are less of a function of the helix voltage.

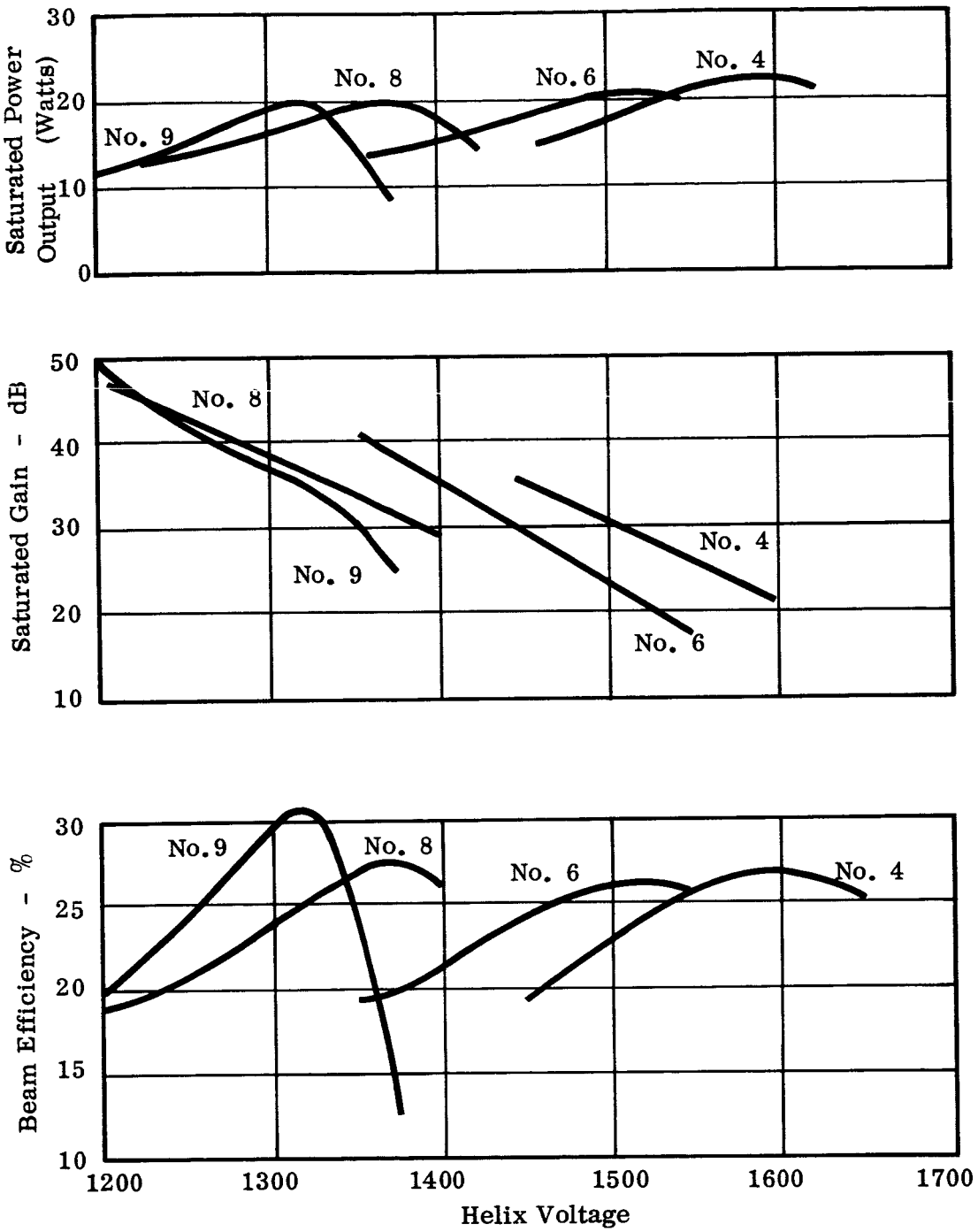

Fig. 5 - Characteristic curves of tube nos. 4, 6, 8, and 9 at 50 mA of beam current. This shows the effect of varying helix design (see table below).

Tube No.	Input Helix	Output Helix	Output Helix Active Length
4	60 TPI	60 TPI	2.67 in.
6	63.5	63.5	2.73
8	58	67.5	2.73
9	58	67.5	3.73

15646

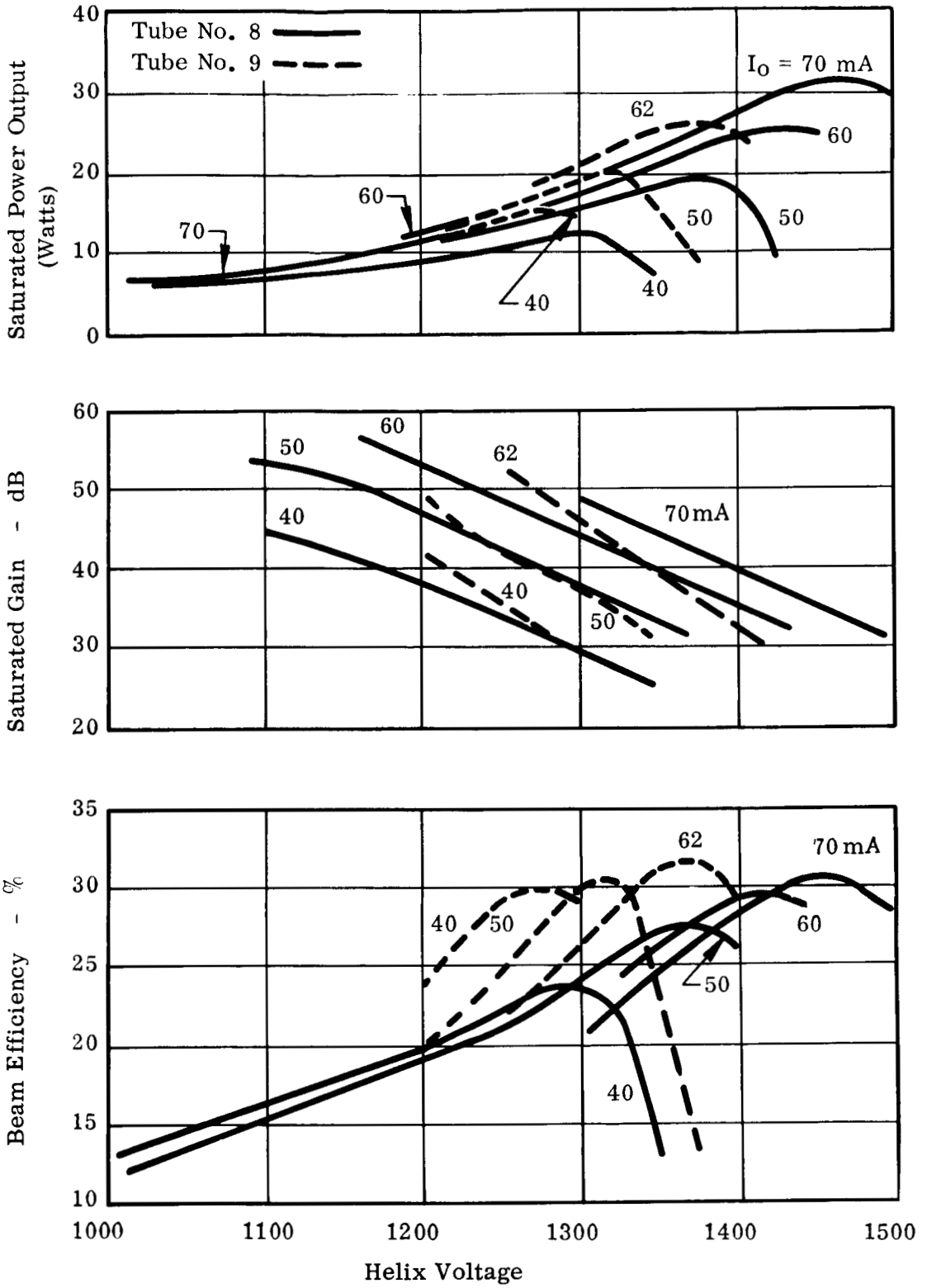

15647

Fig. 6 - Characteristic curves of tube no. 8 and 9 showing shift in performance by adding only output helix length in tube no. 9.

Efficiency and Gain as a Function of Generalized Tube Parameters

The data gathered on tube no. 4 has been thoroughly analyzed, examined, compared and plotted in many ways to determine if any relationships exist between some of the fundamental parameters describing the tube and its efficiency and gain performance. Since overvoltaging plays such an important role in achieving high beam efficiency, an attempt was made to determine if overvoltage could be described in some meaningful way that would then relate to some of the measured characteristics.

Assume that the velocity parameter, b, was actually made up of two components which added arithmetically so that

$$b = b' + b'' \tag{1}$$

The expression that relates beam velocity to the circuit wave velocity still remains

$$\frac{u_o}{c} = \frac{v}{c}(1 + bC) \tag{2}$$

where

u_o is the beam velocity
v is the circuit wave velocity
c is the velocity of light
b is the velocity parameter
C is Pierce's gain parameter[5]

Let b' describe the velocity of the beam which gives maximum small signal gain. Then

$$\frac{u_{sss}}{c} = \frac{v}{c}(1 + b'C) \tag{3}$$

where u_{sss} is the beam velocity for "small signal synchronism" or maximum small signal gain.

Then the term, b'', is a normalized parameter describing the beam velocity in excess of that necessary to give maximum small signal gain.

If the theoretical small signal curves in Birdsall-Brewer[6] are analyzed in terms of equations (1) and (3), a plot of the increasing wave parameter, B, can be developed as a function of b''. These are plotted as the small signal curves in Fig. 7. These curves would be symmetrical about the origin, but are plotted only for positive values of b''. The small signal curves for B form a regular family of curves with the space charge parameter, QC, as a parameter. The term b'' can be seen to have a significance from the standpoint of small signal gain.

Data measured from tube no. 4 has been reduced to the terms of B and b'' for the large signal or saturated gain. With some smoothing of the measured points the curves plotted as the large signal curves of Fig. 7 result. The small and large signal curves tend to approach common values for b'' = 0. Although one would not expect small and large signal values of B to approach the same value, it is significant that they approach the same general location in a similar manner. This give further credibility that the term b'' is also meaningful for large signal conditions.

Various ways of plotting and normalizing efficiency versus b'' were explored and it was found that a significant grouping of the curves could be obtained if beam efficiency were plotted as a function of b'' with C as a parameter. This leads to the plot of Fig. 8 where the actual data points were smoothed to obtain the curves shown.

It now appears that the overvoltage parameter, b'', of a value of about 1.5 marks the region where beam efficiency makes a marked upward turn to achieve values in excess of 30 percent.

It should be noted that the normalization used for this plot may be incorrect. It was found that the size of the electron beam was the least known factor in the calculations. It must be assumed that the diameter of the beam changes as a function of beam perveance because the tube was operated with a fixed magnetic field over a wide range of beam currents and voltages. It is in general not possible to measure the small signal synchronous voltage from the knowledge of which an estimate of the beam diameter can be made. The tube has so much gain at small signal synchronism (greater than 70 dB in most cases) that the tube oscillates strongly except at very low beam currents in the region of synchronism.

This analysis of the controlling parameters of gain and efficiency should be examined in the light of the performance of other tubes and tube types. It does however, present a starting place for designing a tube for high efficiency performance.

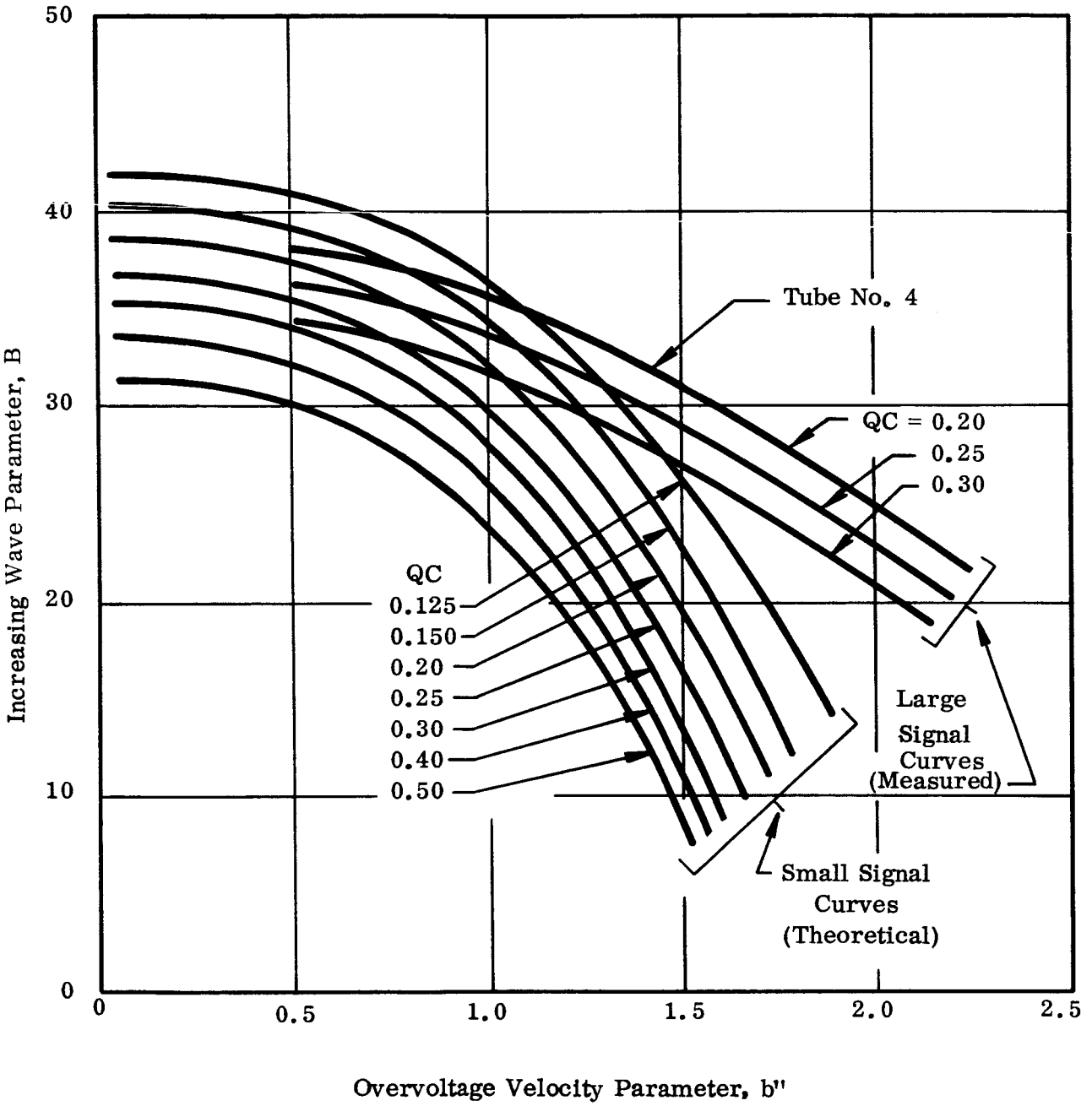

Fig. 7 - Smoothed plot of measured data of large signal B, and theoretical curves (Birdsall-Brewer[6]) for small signal B versus overvoltage parameter, b''.

15632

Fig. 8 - Smoothed plot of experimental data from tube #4 showing apparent relationship of beam efficiency to overvoltage parameter.

Efficiency vs Single Stage Collector Depression

The question is often raised about the relationship between beam efficiency and overall efficiency. Some argue that if the tube is operated below its maximum beam efficiency, the overall efficiency can be recovered by additional depression of the collector voltage. In all our measurements, it has been found that the maximum overall efficiency always occurs at the conditions which also gives maximum beam efficiency. This is shown in the curves of Fig. 9. Here the beam current is held fixed and the overall efficiency is measured as a function of helix and collector voltage. It is seen that maximum beam efficiency and overall efficiency occur under the same conditions. The curves for larger values of helix voltage have been omitted, but both overall efficiency and beam efficiency would fall very rapidly since the 1625 volt curve represents a gain of 20 dB. Any increase of helix voltage makes the gain less than 20 dB which has been previously shown to lead to a very rapid loss of efficiency.

Two Stage Collector Depression

Figure 10 shows a plot of the efficiency performance under both single stage and two stage collector operation. It is seen that there is essentially no difference in the maximum efficiency whether one or two stages are used. This characteristic has become a common occurence on many different tube types once sufficient work has been done on a tube to maximize its single stage efficiency performance. It should be noted, however, that the efficiency does not fall off rapidly with lower collector voltage in the two stage case. This is significant and indicates that the collector 1 is actually absorbing the reflected electrons from collector 2. Why then, does the efficiency not increase? A study of a plot of power dissipation on the various electrodes as a function of collector 2 voltage gives a hint of the difficulty. This is readily illustrated by data from another tube type, the WJ-333, a 4 watt, 4 GHz amplifier which also had a two stage collector which gave no efficiency improvement. A plot of the current distribution among the electrodes is shown in Fig. 11. The cross hatched section of the plot indicates electrons that would not be dissipated on the helix if the slow secondaries were retained within the collector electrode system. The plot of Fig. 11 shows that as the collector 2 voltage passes below that of collector 1 a sudden and abrupt rise in helix current occurs and helix current rises at a more rapid rate below this point than would be predicted by a linear extrapolation of the points above 650 volts. The conclusion is that this added component of current shown as the crosshatched area is due to slow secondary electrons emitted from the inside surface of the collector which

Fig. 9 - Plot showing relationship of overall efficiency to beam efficiency and collector depression.

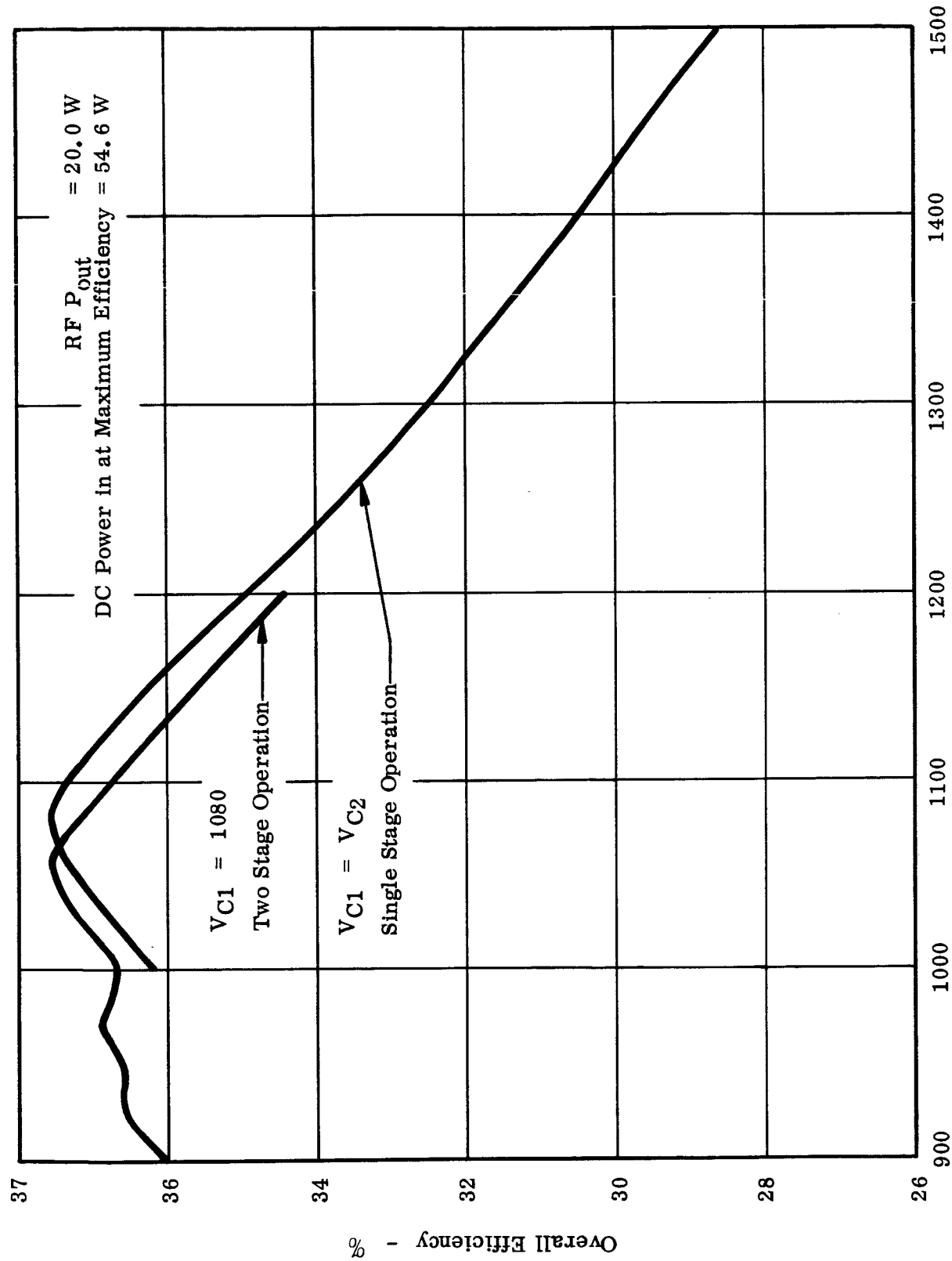

Fig. 10 - Plot of two stage and single stage collector operation showing no efficiency improvement with the 2nd stage operation.

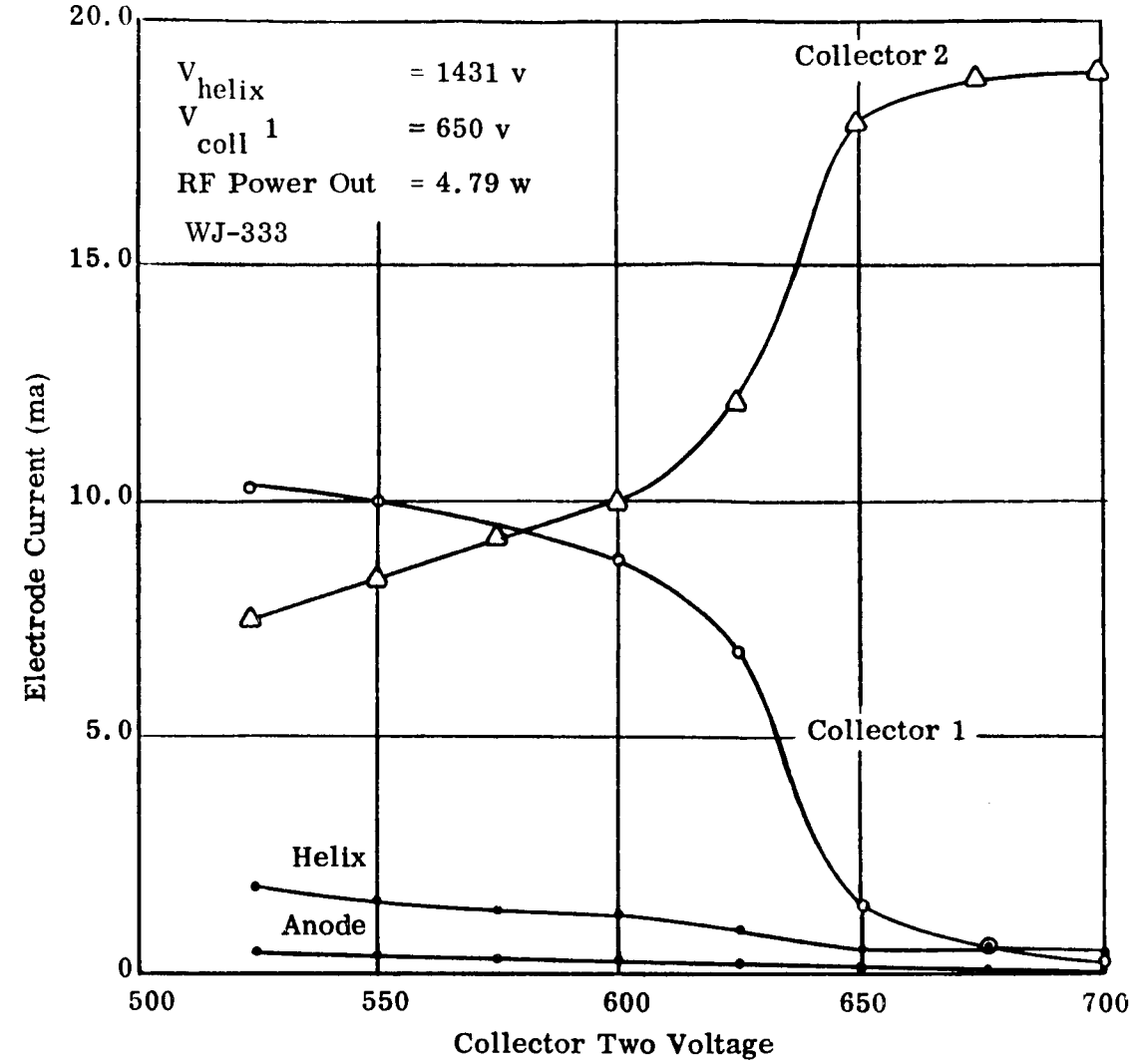

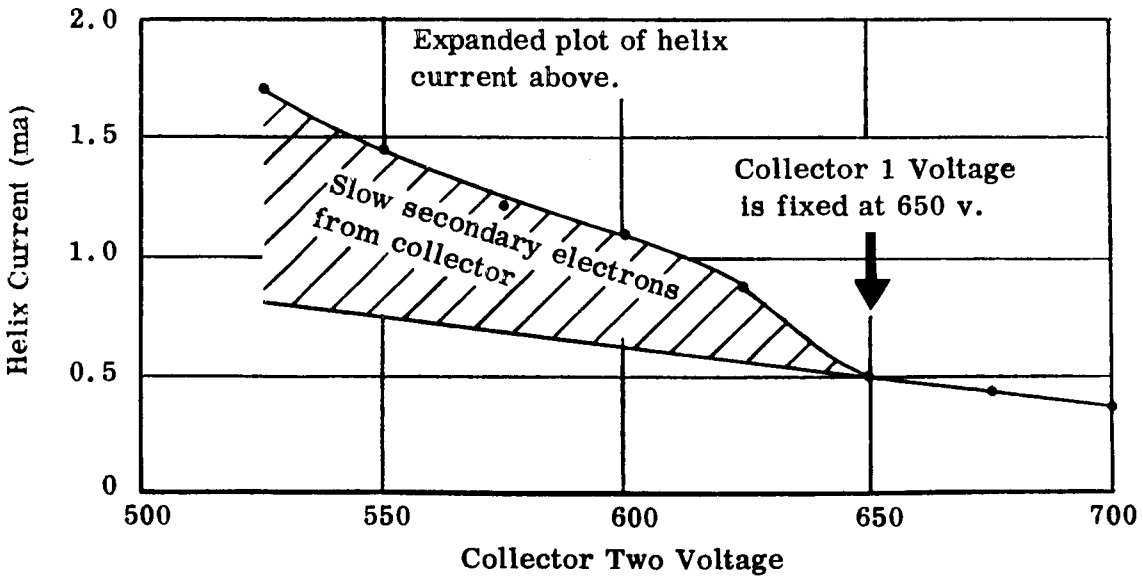

13886

Fig. 11 - Current distribution in two stage depressed collector vs collector 2 voltage. Collector 1 voltage is fixed at a value which gives maximum efficiency in single stage collector. WJ-333.

are focused out through the collector entrance tunnel and onto the helix. These are drawn out of the interior of the collector as soon as the collector 2 potential is lower than collector 1. This sudden rise in current occurs just as the potentials cross. The internal action of the collector is analogous to an electron gun. The secondaries are equivalent to the emitted electrons, the surface of the collector 2 is equivalent to the cathode and the collector 1 is equivalent to the anode. Some of the secondary electrons are then focused out of the collector entrance as if it were the anode hole. This is illustrated in Fig. 12. Performance has been calculated for the case where the secondary electrons in the cross-hatched area of Fig. 11 are assumed to be held within the collector. This hypothetical curve is plotted in Fig. 13 along with the presently measured curves of the WJ-333 for one and two stage operation.

Another problem exists with the use of the two stage collector in conjunction with a space type power supply. Unless an appreciable efficiency improvement is achieved using the two stage collector, the efficiency gain through its use could be canceled out through the additional losses in the power supply. This problem arises from the fact that under no-drive conditions, the traveling-wave tube does not have a velocity spread within the electron beam exiting from the helix. As a result, under no-drive conditions all the electrons are intercepted by the 2nd stage (low voltage stage) of the collector, and no appreciable current reaches the first stage. Under zero load conditions, the 1st stage power supply will charge to the peak value of any switching transient spikes which pass through its rectifiers and the supply section may have its voltage increased by 200 volts. This would ordinarily cause no problem, but in this case all supplies are stacked up in series and helix and anode voltages are in part determined by voltage of this collector section of the power supply. Under no drive conditions, the anode and helix voltage may suddenly rise by 200 volts causing additional cathode current to be drawn as well as applying an incorrect helix voltage. It has happened that the characteristics have shifted sufficiently under these conditions that the tube will not amplify the signal when it is reapplied to the tube input. To prevent the 1st stage collector supply from shifting voltage under these conditions requires the application of a small resistive load across the supply or an output voltage regulation system. Both of these schemes require additional power dissipation and power supply losses. In addition, the regulator scheme adds to the complexity of the power supply and thus tends to reduce its reliability. So, unless the efficiency gained by the use of a two stage collector is appreciable, the added losses and complication of the power supply more than offset the gain made by the collector efficiency.

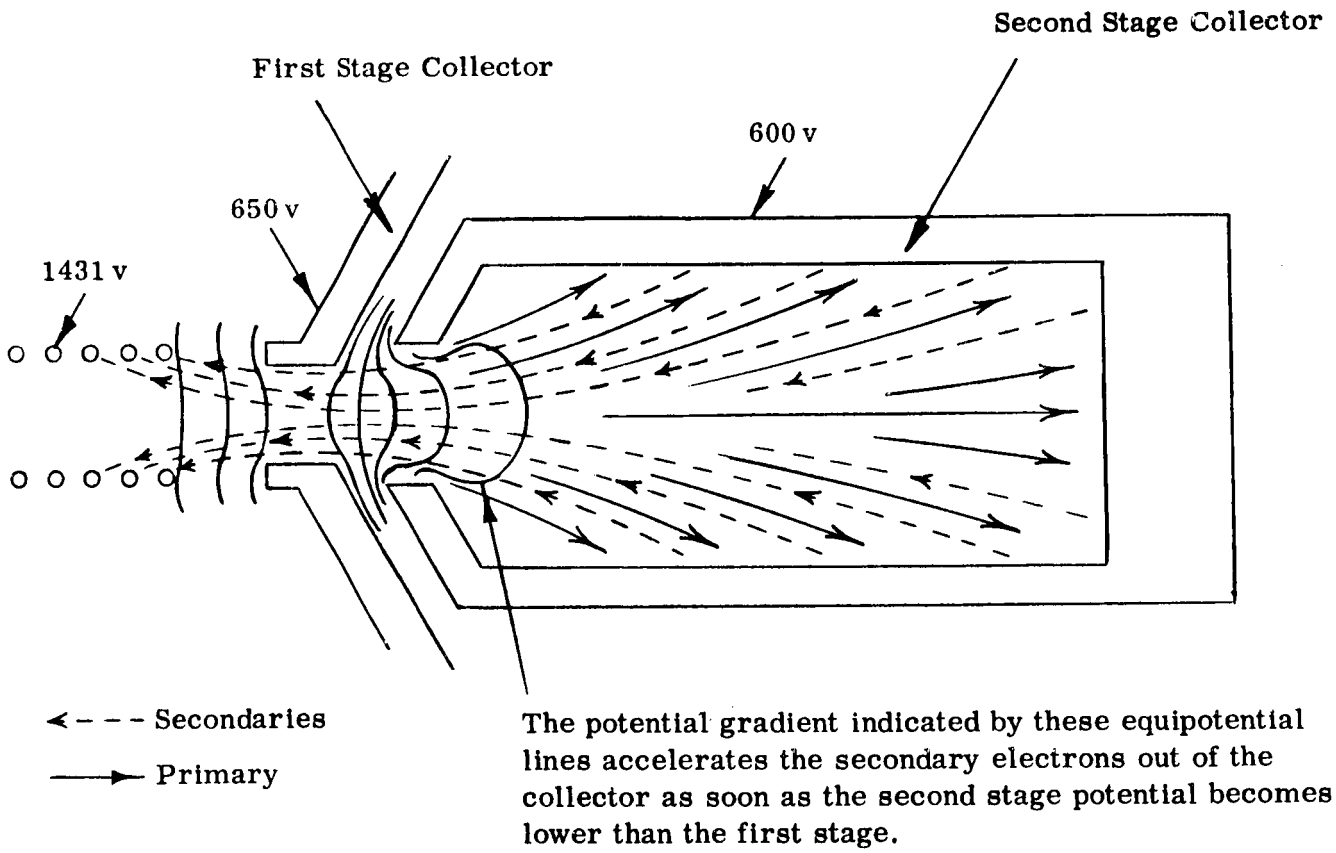

Fig. 12 - Drawing showing potential gradients and source of secondary electrons which raises helix dissipation and prevents correct two stage operation.

13900

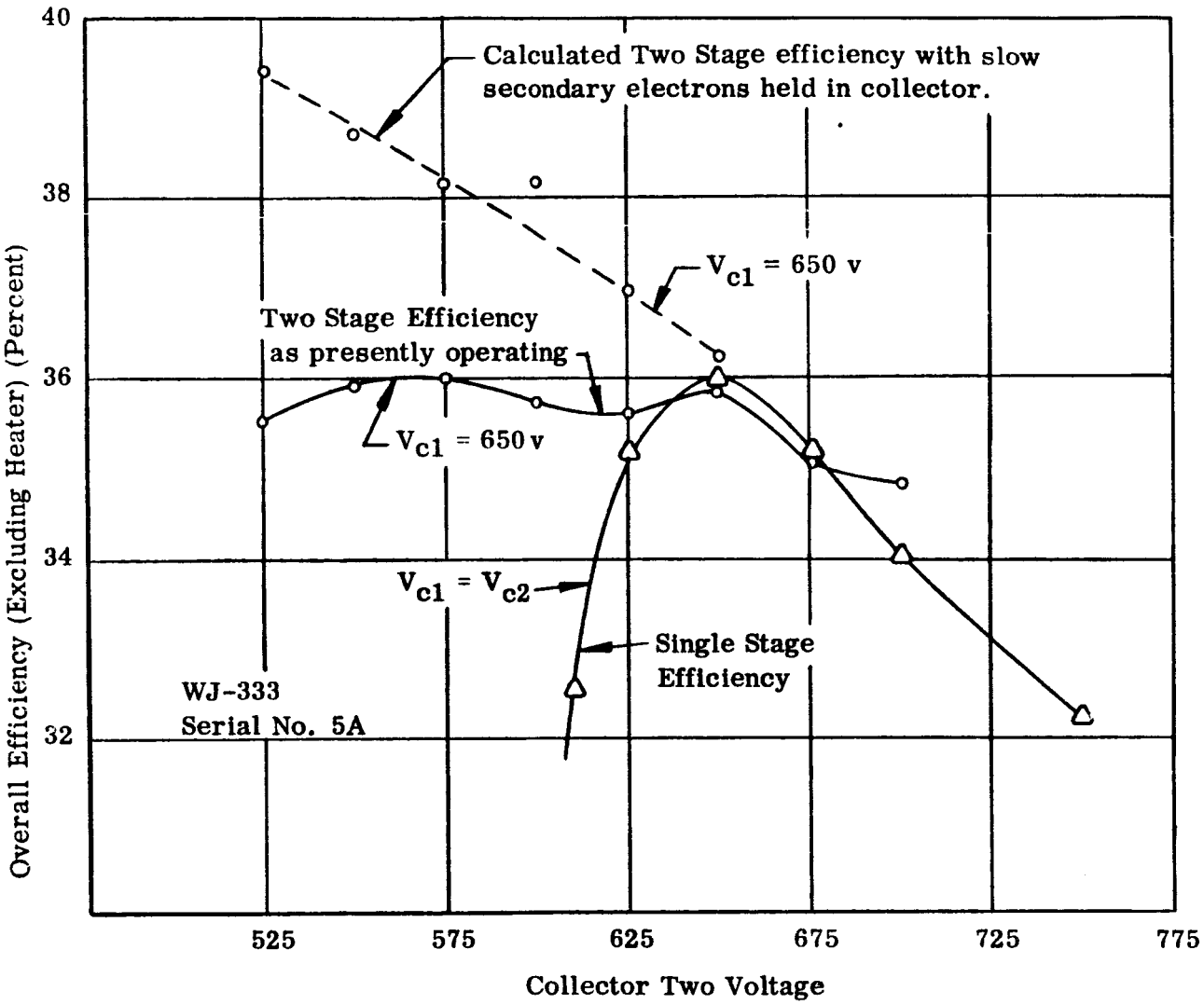

Fig. 13 - Curves showing single and two stage collector performance. Upper dashed curve shows calculated two stage performance if collector is designed to hold slow secondary electrons which are shown as the cross-hatched area in Fig. 11 .

Thus, the fact that two stage collectors are not giving appreciable improvements in the electrical performance of the tube coupled with the fact that the power supply losses and complexity increase when a 2 stage collector is used, make the use of a two stage collector a serious disadvantage.

Broadband Performance

Figure 14 shows typical broadband characteristics that can be obtained with the WJ-274. By merely choosing the proper values of anode, helix and collector voltage the tube can be operated over the range of 20 to 35 watts while at the same time maintaining gain and good efficiency. Overall efficiency (including heater) increases with power level starting at 36.6 percent at the 20 watt level at bandcenter and increasing to 40.2 percent at 35 watts. Actually, the tube can be operated over a wider power range than shown in this curve and similar characteristics to Fig. 14 have been obtained over the 10 to 50 watt range.

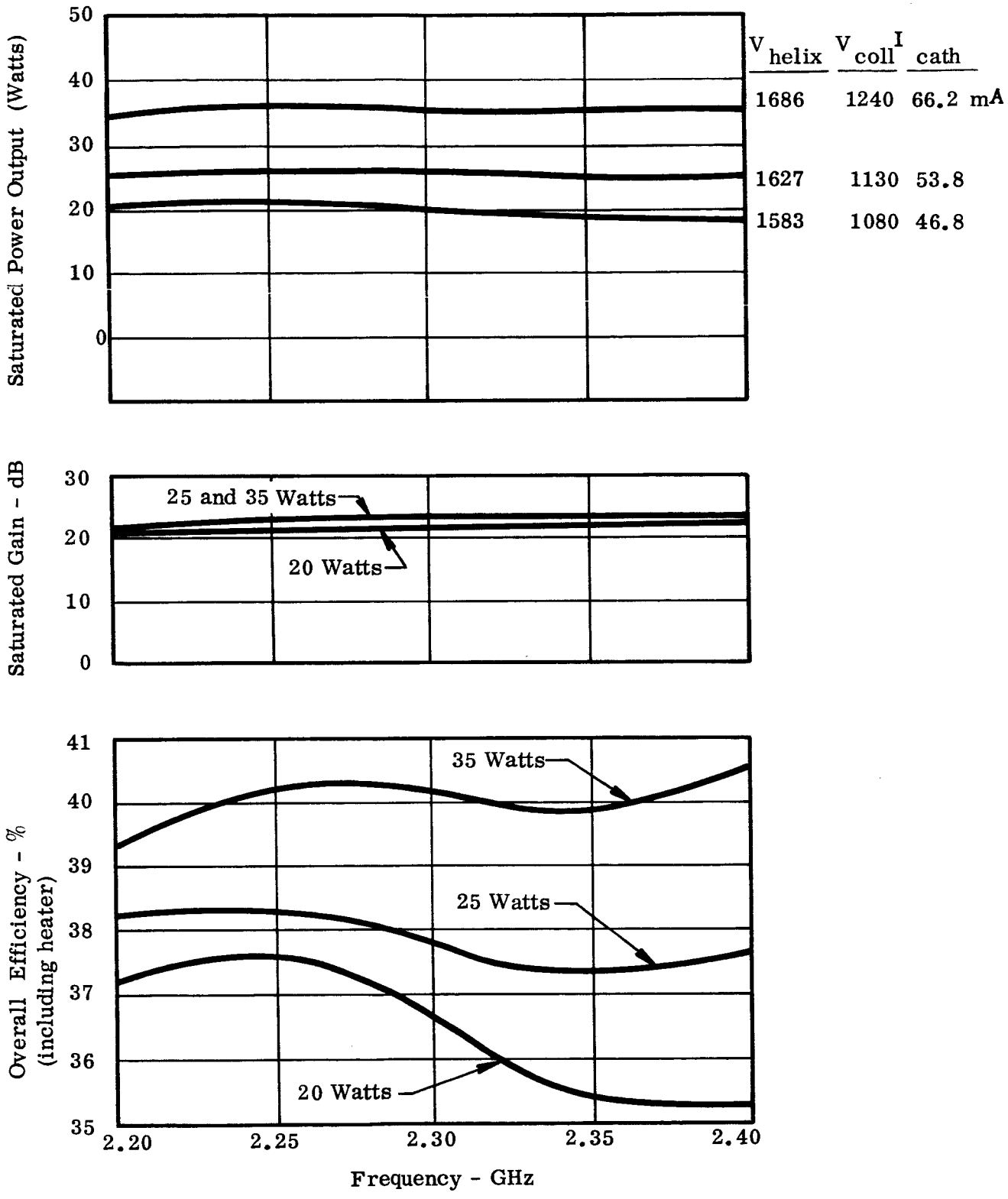

Fig. 14 - Broadband power, gain and efficiency characteristics, showing how the power level can be shifted by programming voltages and current without sacrificing
15650 gain or efficiency.

GENERAL PERFORMANCE OF OTHER CHARACTERISTICS

Power Output vs Power Input Characteristics

Power output vs power input characteristics of a tube operated under large overvoltage conditions are quite different from tubes operated in a more conventional manner. Typically, gain at saturation is larger than at small signal conditions and under certain conditions saturation gain may be as much as 25 dB greater than small signal gain. These tubes are designed to operate almost exclusively at saturation, otherwise there would be no reason for the requirement for high efficiency.

Figure 15 shows the input-output curves of tube no. 4 operating at three different power output levels at a fixed frequency. The saturation efficiencies of all the curves lie in the range of 36.7 to 39.7 percent. The increase in the tube gain from small signal to large signal conditions is seen. In each case, the operating conditions were chosen to give the best efficiency performance at the chosen power level.

Figure 16 shows the input-output curves for a fixed set of operating conditions measured at three frequencies. This is a high efficiency condition chosen for maximum efficiency at 35 watt level at 2.3 GHz. It is interesting to note that the saturated power output level varies very little with frequency while the small signal responses differ very widely.

Figure 17 shows the input-output curves for a fixed set of operating conditions at the same three frequencies as Fig. 16 but with the helix voltage reduced by 80 volts and beam current remaining the same. The overall efficiency has decreased by about 8 percent, the saturated power output has decreased by 5 watts, and the small signal gain has increased to where at 2.3 GHz it is almost the same as the saturation gain. The saturation region of the curve has also broadened so that a wider variation of input signal can be tolerated for a given change in power output.

Figure 18 shows the input-output curves for a tube with an input helix section operating at small signal synchronism. This section of the helix provides a large part of the small signal gain so that even though the output section is effectively operating at large overvoltage, the tube has a more normal response curve. It also raises the overall gain of the tube at saturation, so that saturated gain is 35 dB. The saturation region of the curve is also broadened.

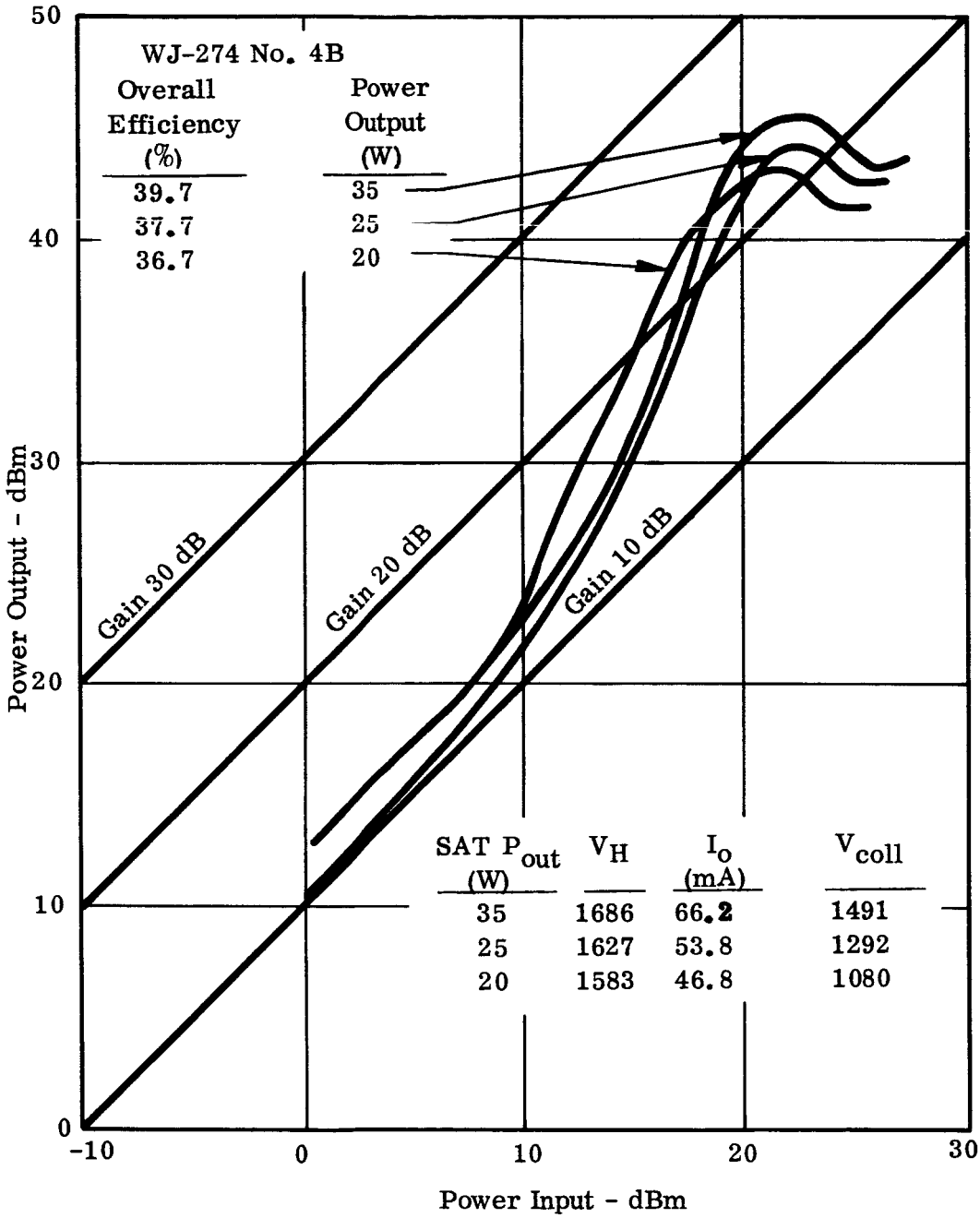

Fig. 15 - Power output vs power input curves at three power levels. This shows the loss in gain at small signal conditions because of large overvoltaging.

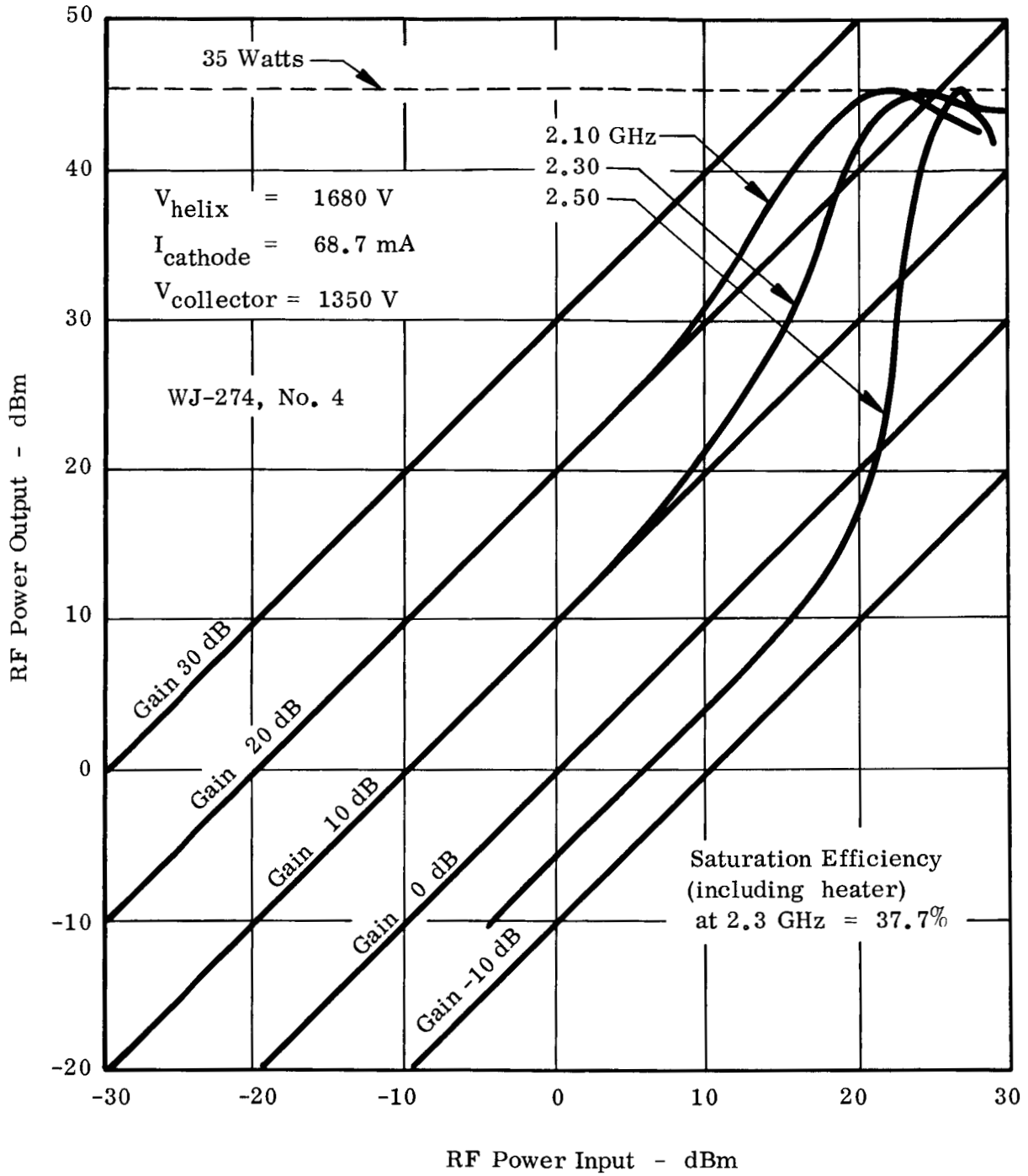

15651

Fig. 16 - Power output vs power input with maximum efficiency at 2.3 GHz and 35 watts power output.

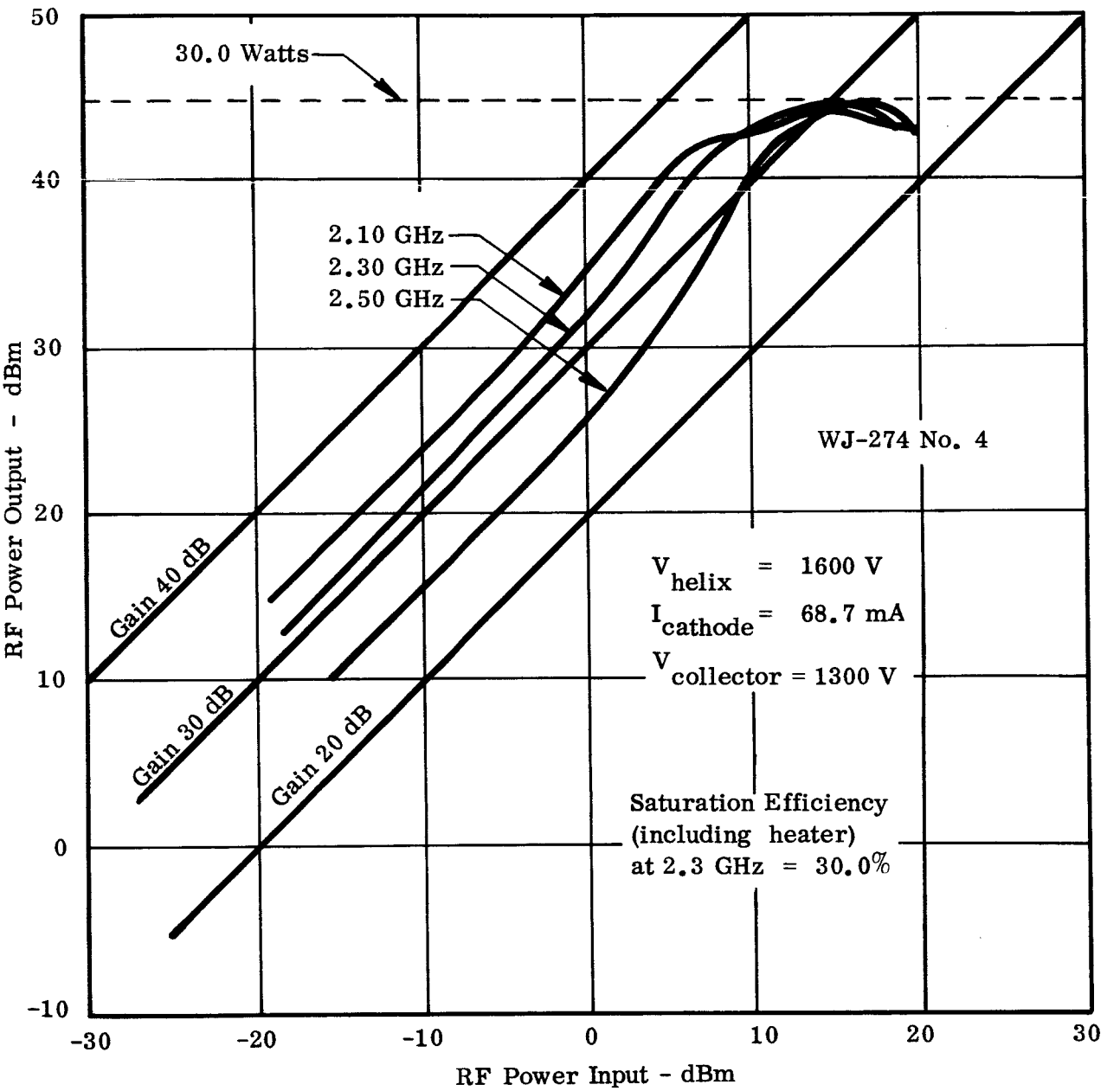

15652

Fig. 17 - Power output vs power input with less overvoltaging and lower efficiency than Fig. 16.

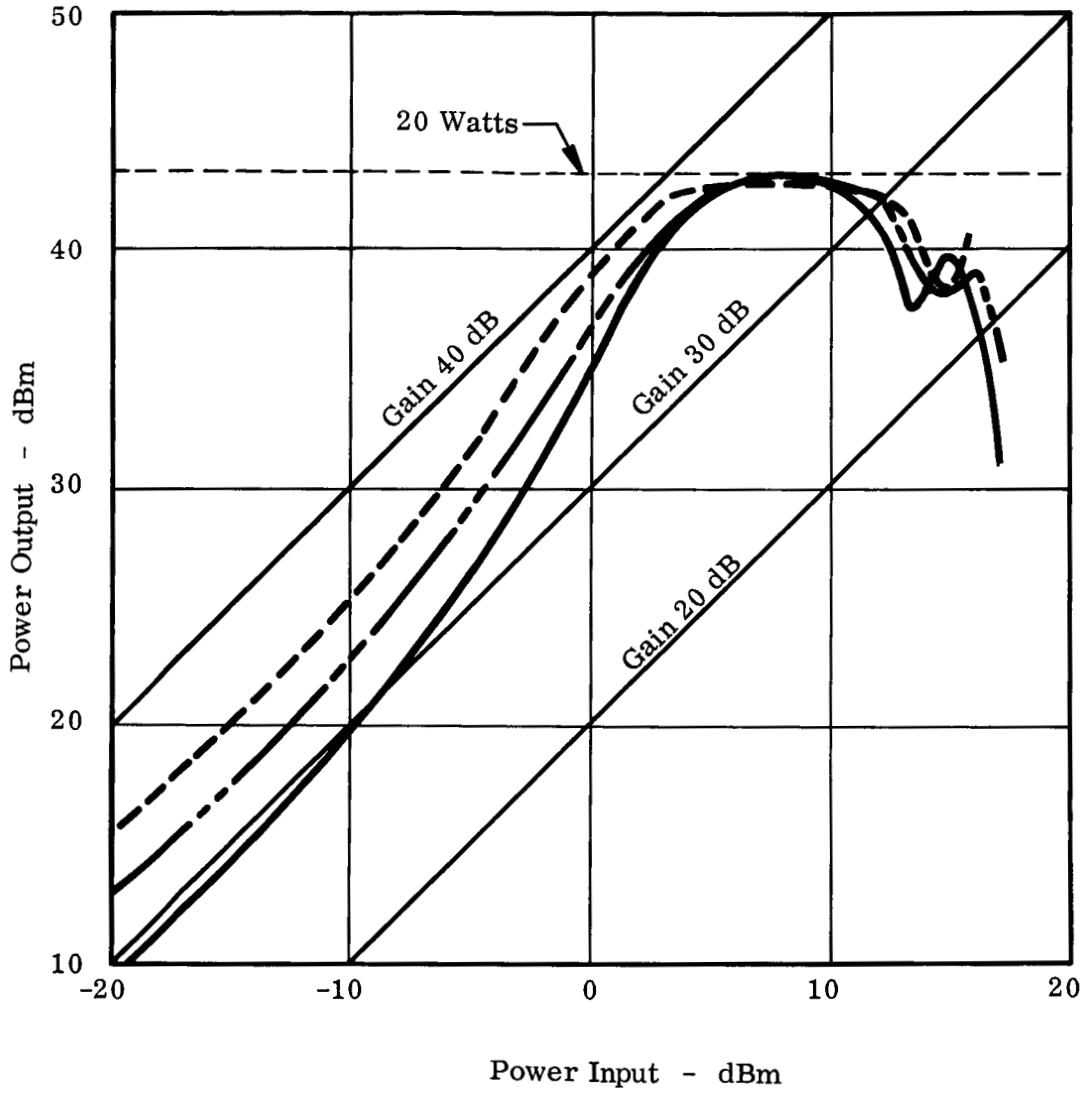

15653

Fig. 18 - Power output vs power input for a tube with additional synchronous helix length ahead of attenuator.

Noise and Spurious Response Performance

Noise requirements for space communication systems have come to place more emphasis on the absolute level of noise power at the tube output than on such characteristics as noise figure. This is because the spacecraft usually has an extremely sensitive receiver operating at a nearby frequency. Since transmitting and receiving functions usually take place simultaneously and often using a common antenna, the tube noise output characteristics cannot be ignored. Noise figure usually has significance only at the input of sensitive receiving systems. Sometimes a large signal noise figure (depending on its definition) has meaning for multiple repeater systems where the noise on the carrier can be additive. We will ignore the noise figure concept for the moment and look at only the noise output power.

Figure 19 shows the noise output of tube no. 4 for the conditions of no drive and saturated drive. This shows that under saturated conditions the noise measured in a 1 MHz bandwidth is approximately 80 dB below the carrier level. The receiver used for this measurement has sufficient skirt selectivity that it can be tuned to within 10 MHz of the carrier before the receiver begins to respond to the carrier signal. The effective receiver bandwidth is 2.8 MHz so that the actual noise level out of the tube and measured at the receiver input is 4.5 dB. higher and then is corrected by this amount to normalize it to a 1.0 MHz bandwidth. No coherent spurious responses are visible across this frequency range at this uncorrected signal level of approximately 76 dB below the carrier up to within 10 MHz of the carrier.

Closer examination of the signal within this 10 MHz region on either side of the carrier requires special receiving equipment which Watkins-Johnson Company does not have at this frequency range. Measurements made at X-band on a complete amplifier system which included tube and solid state power supply with a synchronizer stabilized signal generator-receiver system showed that spurious coherent responses close to the carrier were all due to power supply ripple frequencies and harmonics which give frequency modulation sidebands to the carrier. In the case of the X-band unit, the largest sideband was 66 dB below the carrier and this was caused by ac heater voltage and a common heater-cathode lead and junction within the tube envelope. This situation does not exist on the WJ-274.

The noise output level from the tube under no-drive conditions is seen to be about 105 dB below the carrier. This noise level is usually of no consequence except to meet "key up" noise conditions of various Mil Specs. Both MIL-I-26600

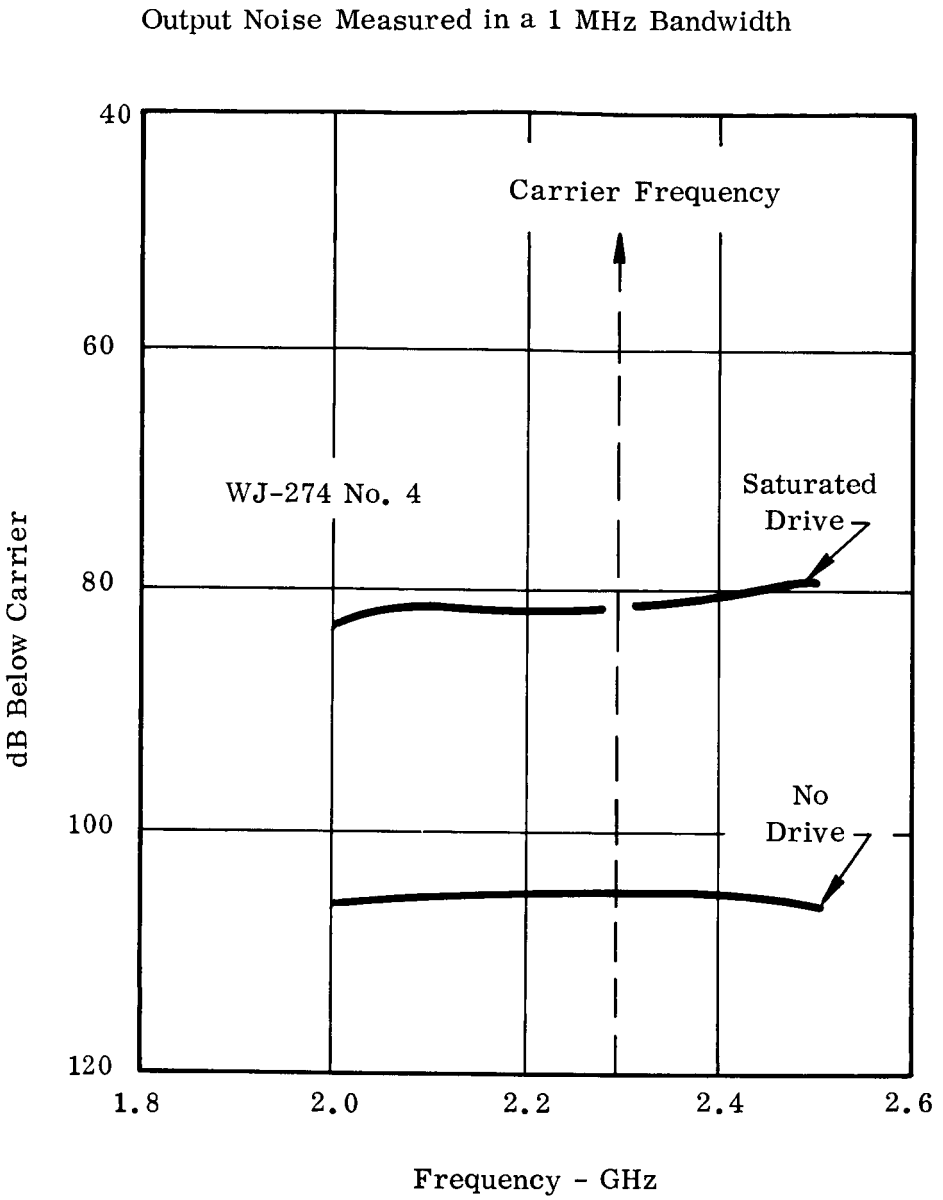

15630

Fig. 19 - Noise output of tube No. 4 measured in a 1 MHz bandwidth under no drive and saturated drive conditions. Carrier frequency is 2.3 GHz. The receiver could reject carrier signal up to within 10 MHz of carrier.

and MIL-I-6181 effectively require that this "key up" noise be at least 90 dB below carrier measured in a 1 MHz bandwidth. The tube meets this requirement with about a 15 dB margin.

Figure 20 shows the noise output variation measured at a typical receiver frequency of 2180 MHz as a function of the input drive level to the tube. The fundamental power output variation is also plotted as a function of input drive level. For an 18 dB range of input drive below the saturation drive level, the noise is at least 76 dB below the carrier. The noise shows a curious peak of 60 dB below carrier for a drive level which is 7 dB greater than the saturation drive level. This peak corresponds to a dip in the fundamental power output curve. It should be noted that this measurement was made on a tube which had more gain ahead of the attenuator than tube no. 4 and thus has about 7 dB more noise output at saturation. It is the same tube as measured in Fig. 18 and thus has a gain at saturation which is 15 dB greater than tube no. 4.

Although noise figure of these tubes is not a truly significant requirement since they are not involved in receiving systems, noise figure performance is plotted in Figs. 21 and 22 for the sake of completeness. It also gives an insight into what factors are significant in determining noise figure. Fig. 21 corresponds to WJ-274 no. 8 and Fig. 22 corresponds to WJ-274 no. 4. The power output, gain and beam efficiency which correspond to Figs. 21 and 22 can be determined from Figs. 6 and 4 respectively.

It is interesting to note that for both tube nos. 4 and 8 that when the gain of the tube was 37 to 38 dB, noise figures of 22 to 23 dB were obtained. However, under the large overvoltage conditions for maximum efficiency, the tube gains were much lower and the noise figure suffered accordingly. This is primarily due to the gain ahead of the attenuator in the input helix section of the tube. It is in this section of the tube where the noise figure is established, and when the gain in this section of the tube is low, the signal is not efficiently transferred on to the beam. Beam noise, which is determined in the electron gun, is already established on the beam before entering the input helix. Thus gain of the input section is the determining factor on the relative rate of buildup of signal power to noise power and thus establishes noise figure. If the noise figure performance were important, then the tube design should be changed to increase the gain of the input helix section.

As a point of interest, other tubes in other frequency ranges exhibit a best noise figure of 22 to 23 dB under operating conditions where they have adequate gain in the input helix section. Two examples of these are the WJ-333, a 4 watt, 4 GHz tube and the WJ-251, a 3 watt, 7-8 GHz tube.

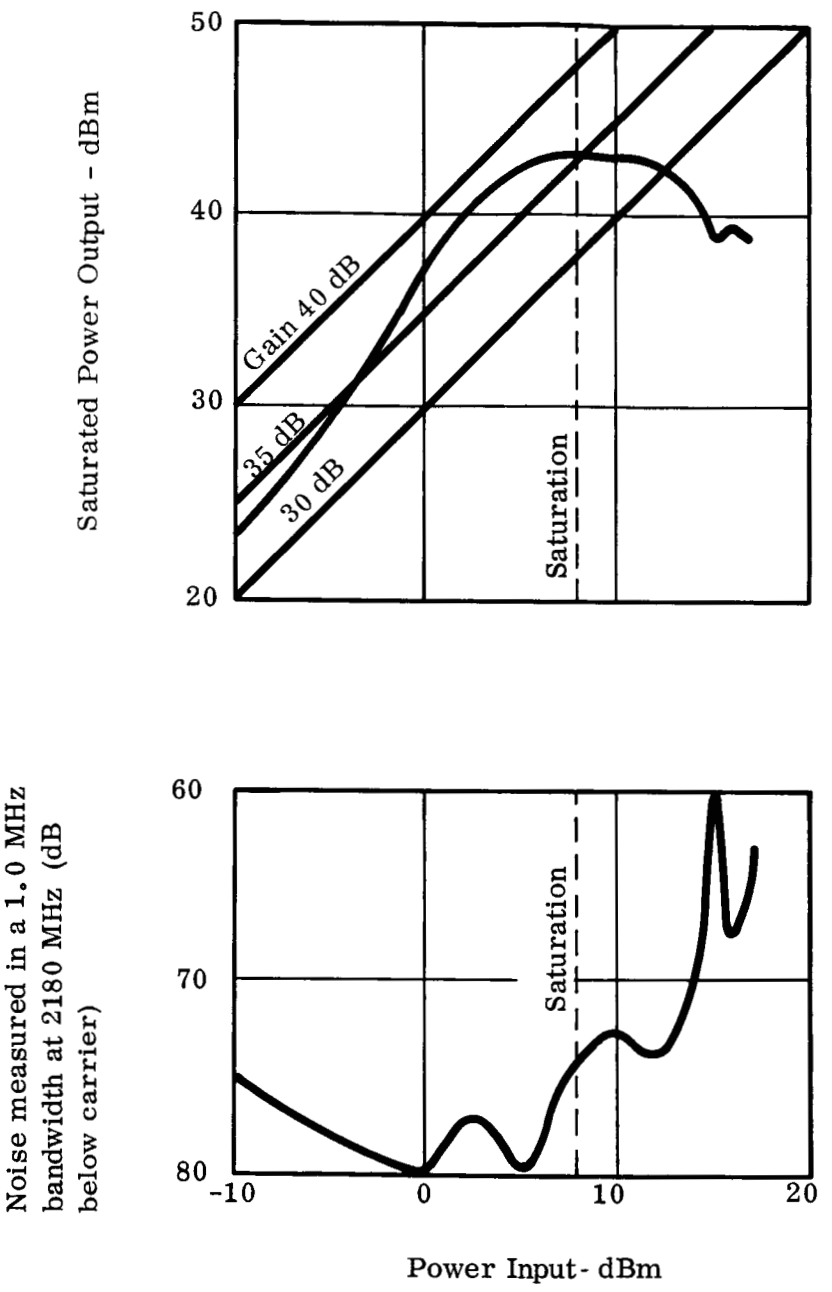

15631

Fig. 20 - Curves showing noise output and signal output from tube as a function of input power. This tube has more gain ahead of attenuator than tube No. 4. It exhibits a higher noise level at saturation.

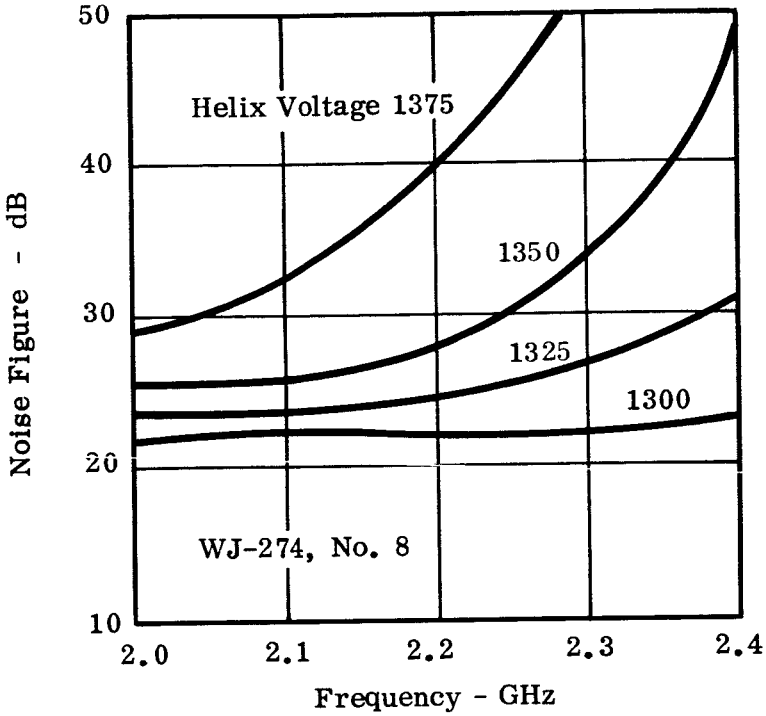

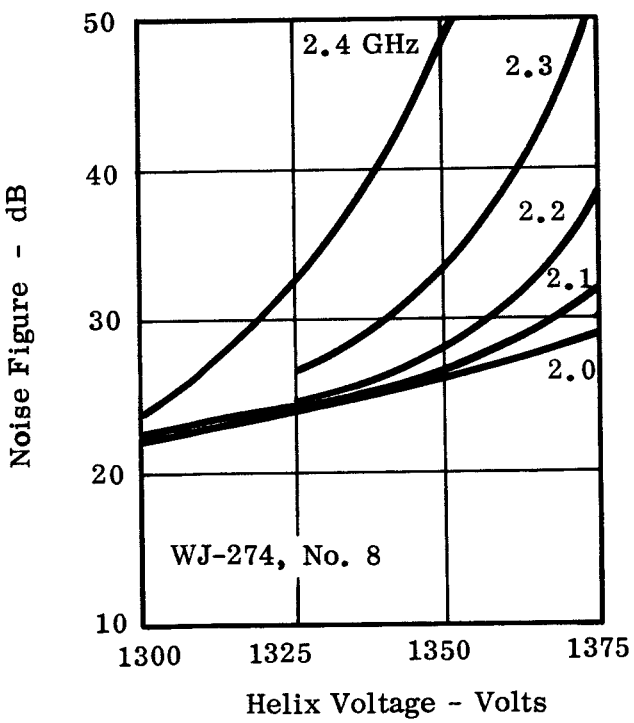

Fig. 21 - Small signal noise figure vs frequency and helix voltage. Beam current = 50 mA.

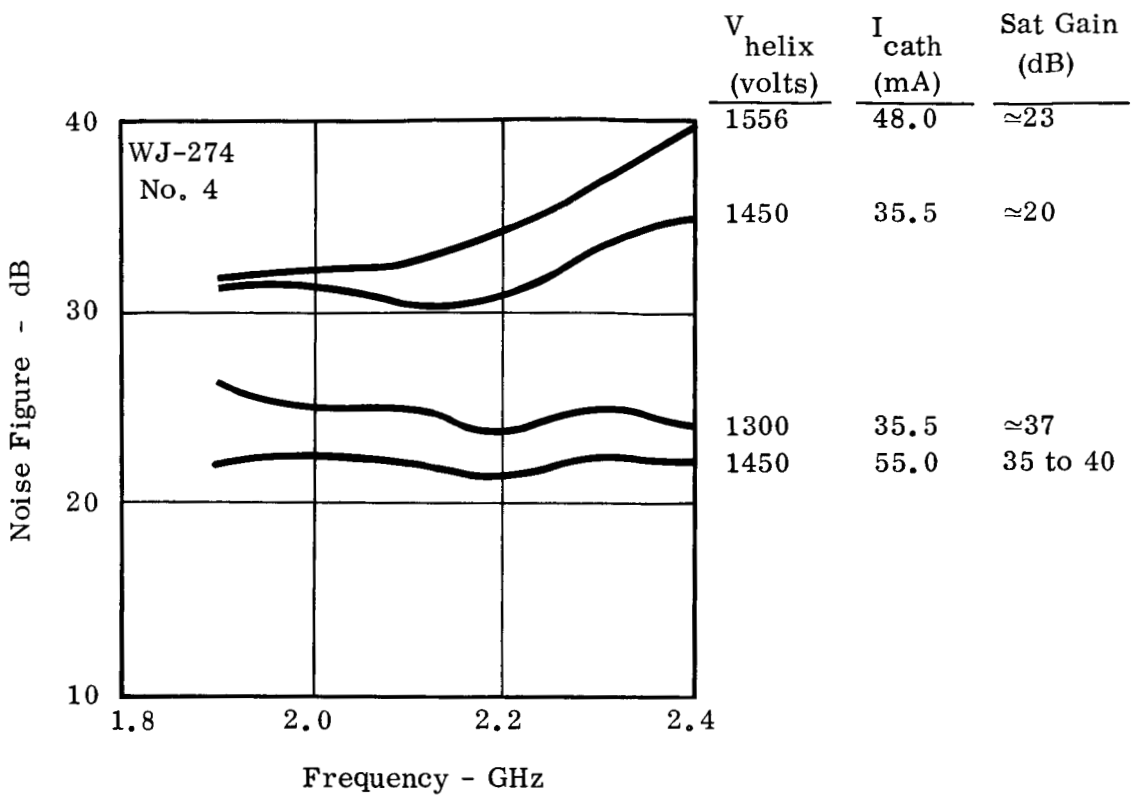

15655

Fig. 22 - Small signal noise figure vs frequency for WJ-274 No. 4.

AM to PM Conversion

Figure 23 relates AM-PM conversion to the beam efficiency of the tube. This data was taken at a fixed beam current. Power output, beam efficiency and overall efficiency are really functions of the helix voltage as the independent variable, but it was plotted in this way to make the explanation clearer.

The phase of the output RF voltage of the tube is related to the phase of the electron bunches in the beam. The phase of this circuit RF voltage does not follow the phase of the beam bunch at the end of the helix exactly because it represents the integrated effect of coupling to the space charge fields of the bunches over a length of helix. However, when the phase of the electron bunch lags, the phase of the voltages tends to lag also. Thus in a tube which attains high overall efficiency by attaining a high beam efficiency, slowing of the electron bunches will be large (which represents a large transfer of energy to the circuit waves) and the resulting phase lag of the output RF voltage wave will be large.

AM-PM conversion is defined as the ratio of the phase shift of the output voltage to the dB change in input drive power. Thus, as the operating parameters of a tube are changed to increase its beam efficiency, the phase lag of the RF output voltage will be greater per dB change of input drive signal. This is borne out by Fig. 23. As beam efficiency is increased, AM-PM conversion increases rapidly to large values. This is a consequence of the miniature tube design. C, the gain parameter, is made large (i.e., >0.1) to get as much gain per unit length as possible so that the tube can be short. Large C means also large QC which in turn means more slow electrons are present. This prevents large efficiency improvement factors by collector depression and means that overall efficiency improvement must come from beam efficiency improvement. Thus the resulting efficiency improvement by overvoltaging results in large values of AM-PM conversion.

In typical tube designs at X-band, for example, lower C designs must be used because of focusing limitations which force lower beam perveance to be used. As a result, QC values are lower and greater collector depression is realizable and good efficiency can still be achieved. The tubes do not have an excessive length because wavelength is shorter and the additional number of wavelengths needed to achieve a given gain do not make the tube any physically longer than the S-band region tubes.

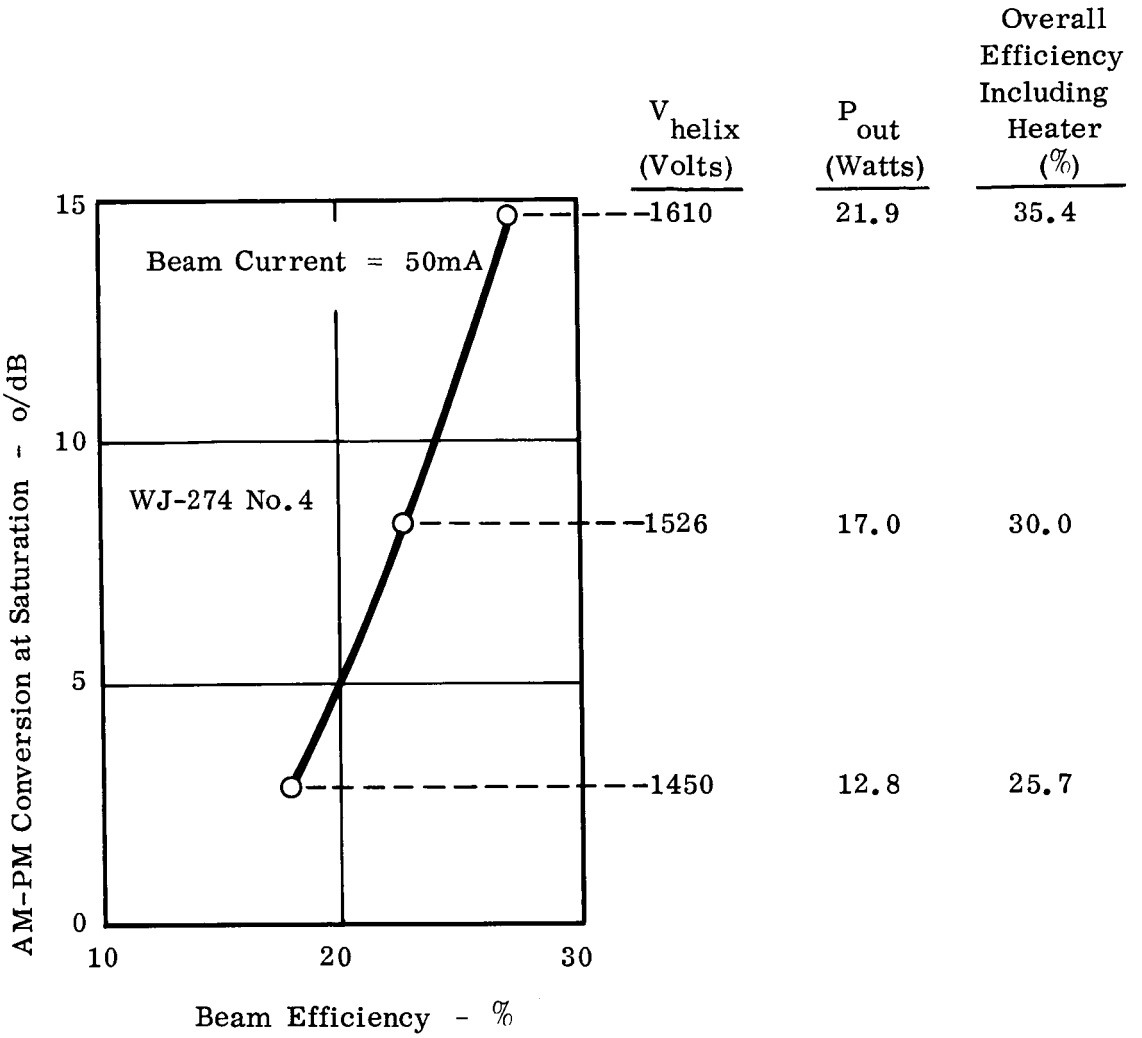

15656

Fig. 23 - Plot of AM to PM conversion at saturation vs beam efficiency.

Phase Linearity

Fig. 24 is a plot of relative output phase difference as a function of frequency. It is really a measure of the phase difference between the tube output and that of a reference passive phase element of supposedly the same electrical length. The electrical length obviously was not the same or the phase difference line would have been horizontal. However, what is important is that the tube output phase vs frequency be as close to a straight line as possible. A straight line of the average slope of the phase curve has been drawn as a reference. It can be seen that over the frequency range from 2280 to 2440 MHz the departure from a straightline is no more than 1.5 degrees. The specifications allow a 3.0 degree departure per 10 MHz. If the best straight line fit over any 10 MHz range were made, there would be no distinguishable phase difference between the tube curve and the straight line segment.

It should be noted that this is a difficult measurement to make. It must be made in a coaxial system which includes a liberal quantity of connectors and adapters all of which introduce frequency sensitive phase errors. This probably accounts for kink in the phase curve in the vicinity of 2270 MHz. When measuring over a wide frequency range such as for this plot, the smoothest data was obtained for a fixed value of drive power level. Since the gain of the tube varies somewhat over this range, an additional slowly changing phase shift is superimposed due to AM-PM conversion.

Phase Shift vs Helix Voltage

Figure 25 shows a plot of relative phase shift as a function of helix voltage. At the operating voltage of 1610 volts, the slope is 2.2 °/volt. The output power variation as a function of helix voltage is also plotted.

Intermodulation Products

Figure 26 is a plot of the first order intermodulation products and the fundamental signals as a function of total input drive level. This is equal amplitude data, i.e., both fundamental signals, f_1 and f_2, are applied to the tube input at the same amplitude. Unfortunately, no data was taken under beam current and helix voltage values corresponding to typical operating conditions. Nevertheless, the data obtained is probably very indicative of a typical performance. It is seen that the difference between the first order intermodulation products, $2f_1 - f_2$ and $2f_2 - f_1$, and the individual fundamental signals at saturation is only about 5 dB. In tubes operating at beam efficiencies of 20 percent and below, the difference between the fundamentals and the first order products is typically 12 dB. So it is seen that a price is paid for operating efficiency in terms of the amplitudes of the intermodulation products.

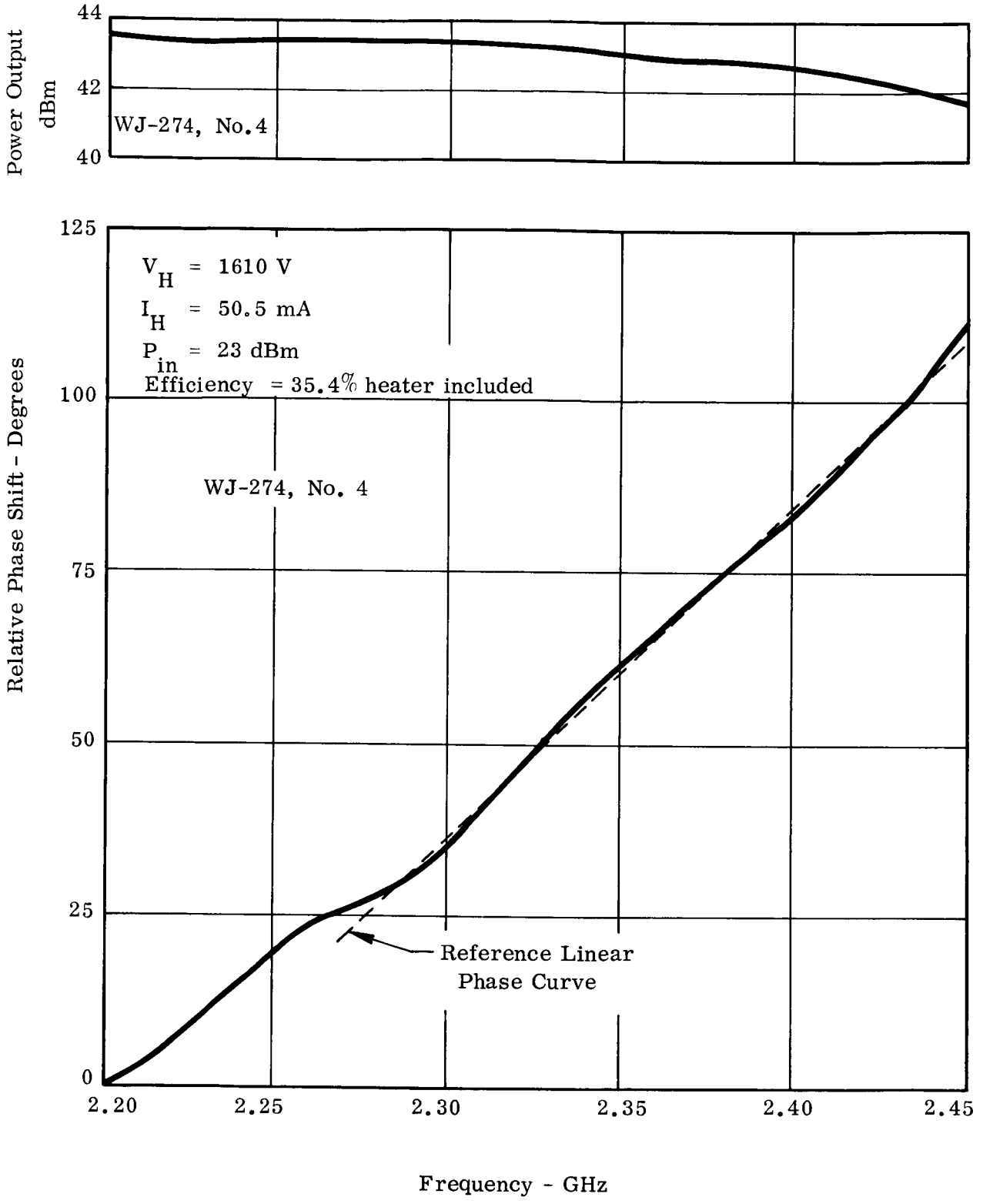

Fig. 24 - Relative phase shift vs frequency for fixed drive level.

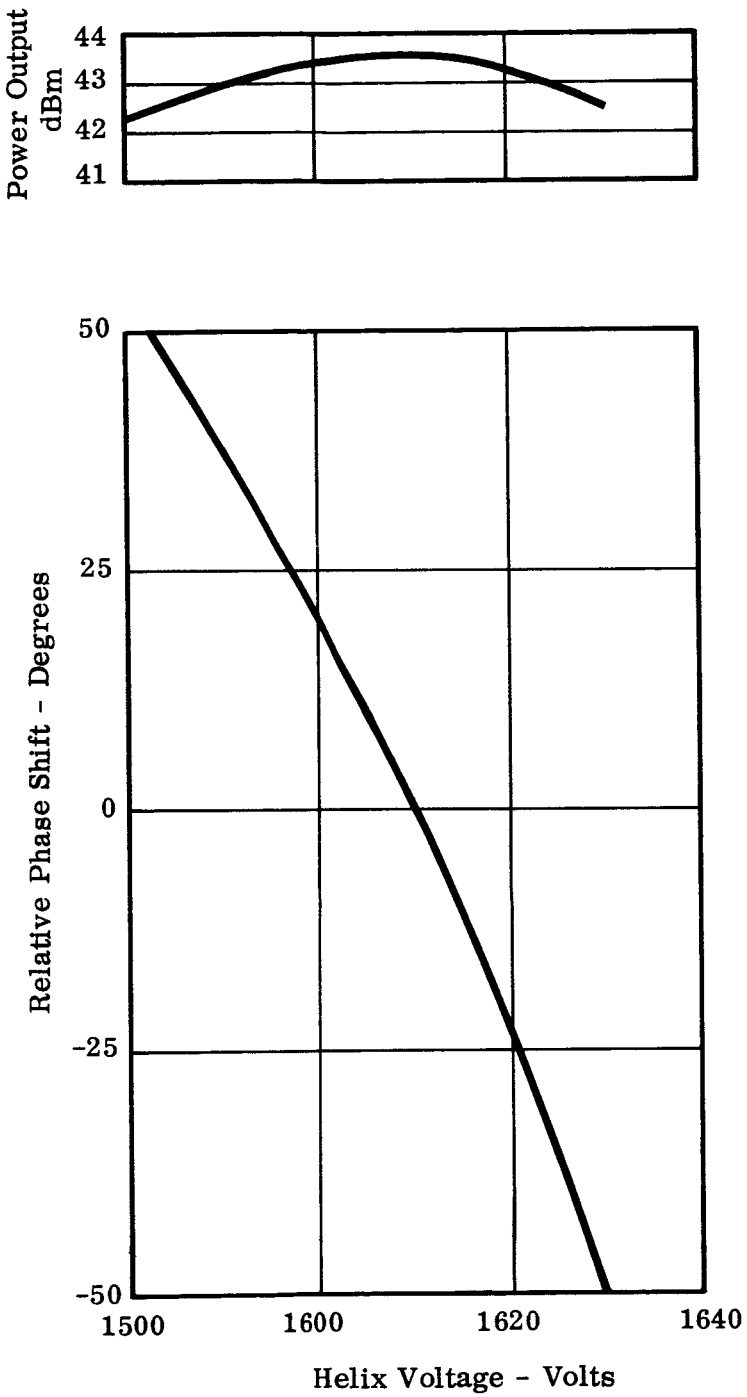

Fig. 25 - Phase shift and power output vs helix voltage. WJ-274 No. 4

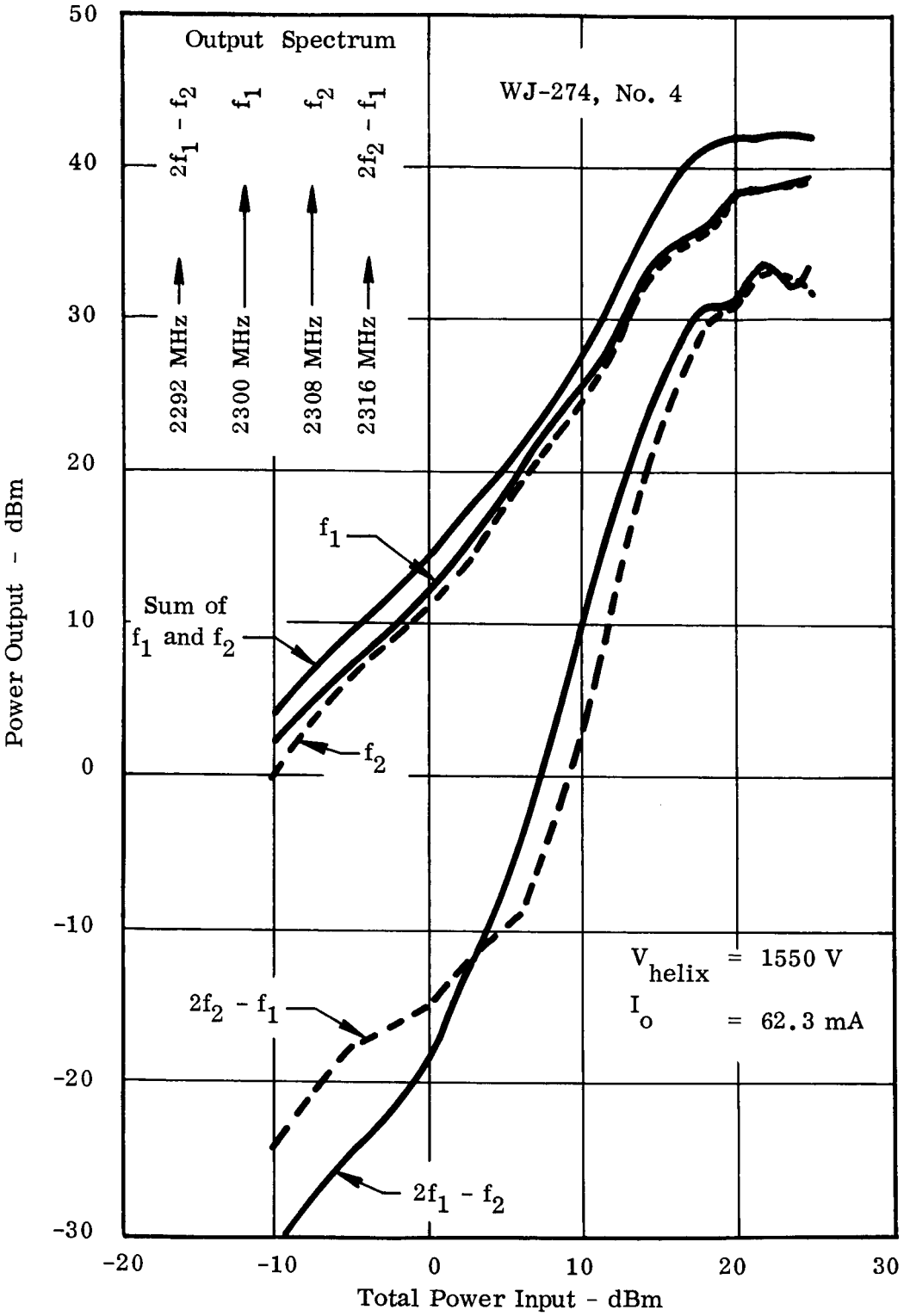

15659

Fig. 26 - Two signal equal amplitude intermodulation product data. No data was taken under normal voltage and current conditions.

PHYSICAL CONFIGURATION

Figure 27 shows a photograph of the WJ-274 showing a completed tube with magnets and also a body with cathode-header and collector subassemblies ready for final assembly. The subassemblies are joined to the ends of the body by simple and rapid RF induction brazes. This method of joining also allows these parts to be simply removed if they need repair or replacement. Pumping of the tube is accomplished through the collector end which allows the insulating header at the gun end to be a simple part with vacuum seals having large metallized areas for reliability.

Body Assembly

Figure 28 shows a breakdown of the body subassembly with its component parts. The main central section of the body is made up of a piece of thin wall tubing onto which is brazed a series of pole pieces and spacer rings. This unit becomes one solid and integral assembly with the pole pieces and spacer rings thermally joined to the tubing and to one another. This makes a body which has a large heat carrying capacity and which will have no microscopic vacuum gaps which could lead to heat transfer problems when operating in the vacuum of space. This is a major advantage of the brazed assembly. The pole piece and central body section is made as one unit. It subsequently has some machining done and then the gun and input transmission line subassembly and output transmission line and collector end pole-piece cup subassembly are joined in a subsequent brazing operation. This then constitutes the body subassembly. It is a mechanically rugged assembly. It contains no potentially weak vacuum joints where thin ceramic parts are used as part of the body. Where ceramic seals are used it separates their function into extremely reliable types of seals and if they serve as dc insulator they do not also have to double as RF window.

The upper body subassembly in the photograph shows the RF window mounts and transmission line in place. Just above the right hand window can be seen the window-stripline subassembly before insertion into the body. This brazes directly into the threaded window cup and the end of the stripline also brazes directly onto the end of the helix wire. All these brazed joints in the transmission line from window to helix give reliable and low loss connections and do not depend upon the unreproducible RF connections of spot welded joints. The window-stripline combination is carefully designed to maintain a 50 ohm characteristic impedance right down to the first spread turn of the helix impedance transformer. The assembled window is designed to screw directly into the back of a specially adapted TNC or OSM connector.

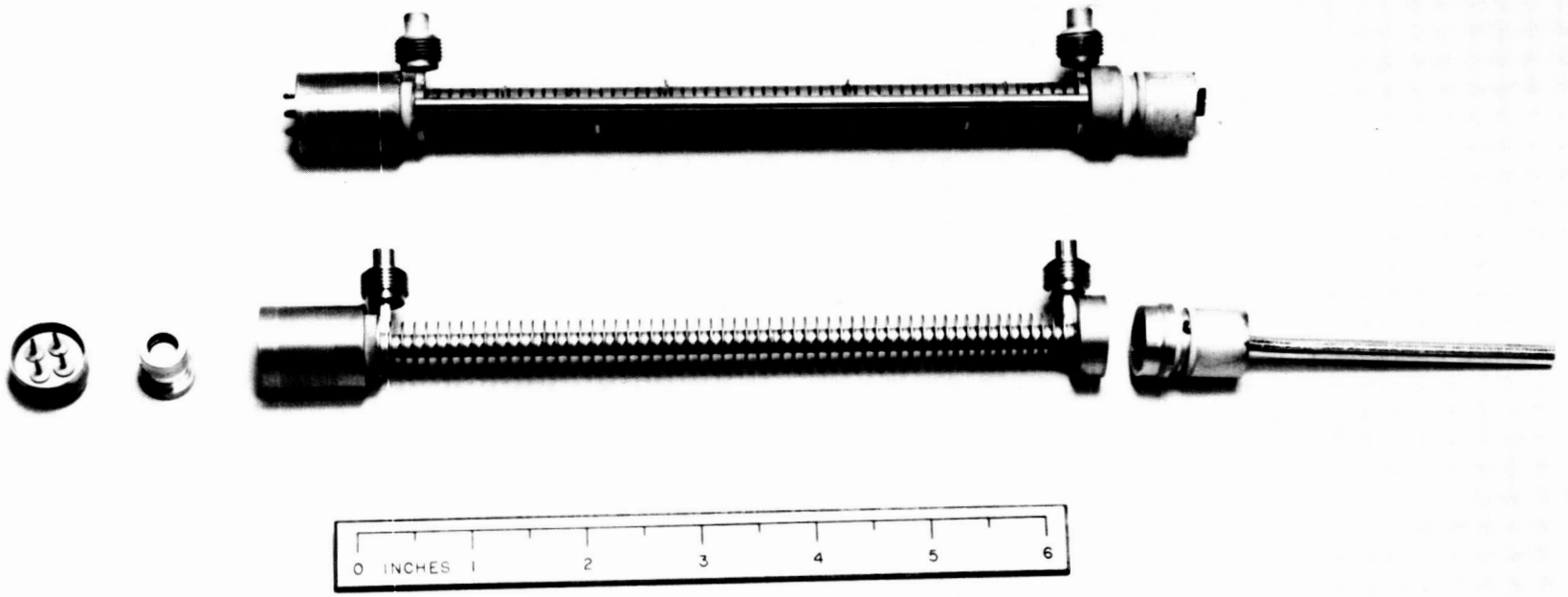

WATKINS JOHNSON

3173-1

Fig. 27 - Photograph of the WJ-274 showing a completed tube with magnets in place (above) and a completed body with cathode and header subassemblies to the left and collector subassembly to the right (below).

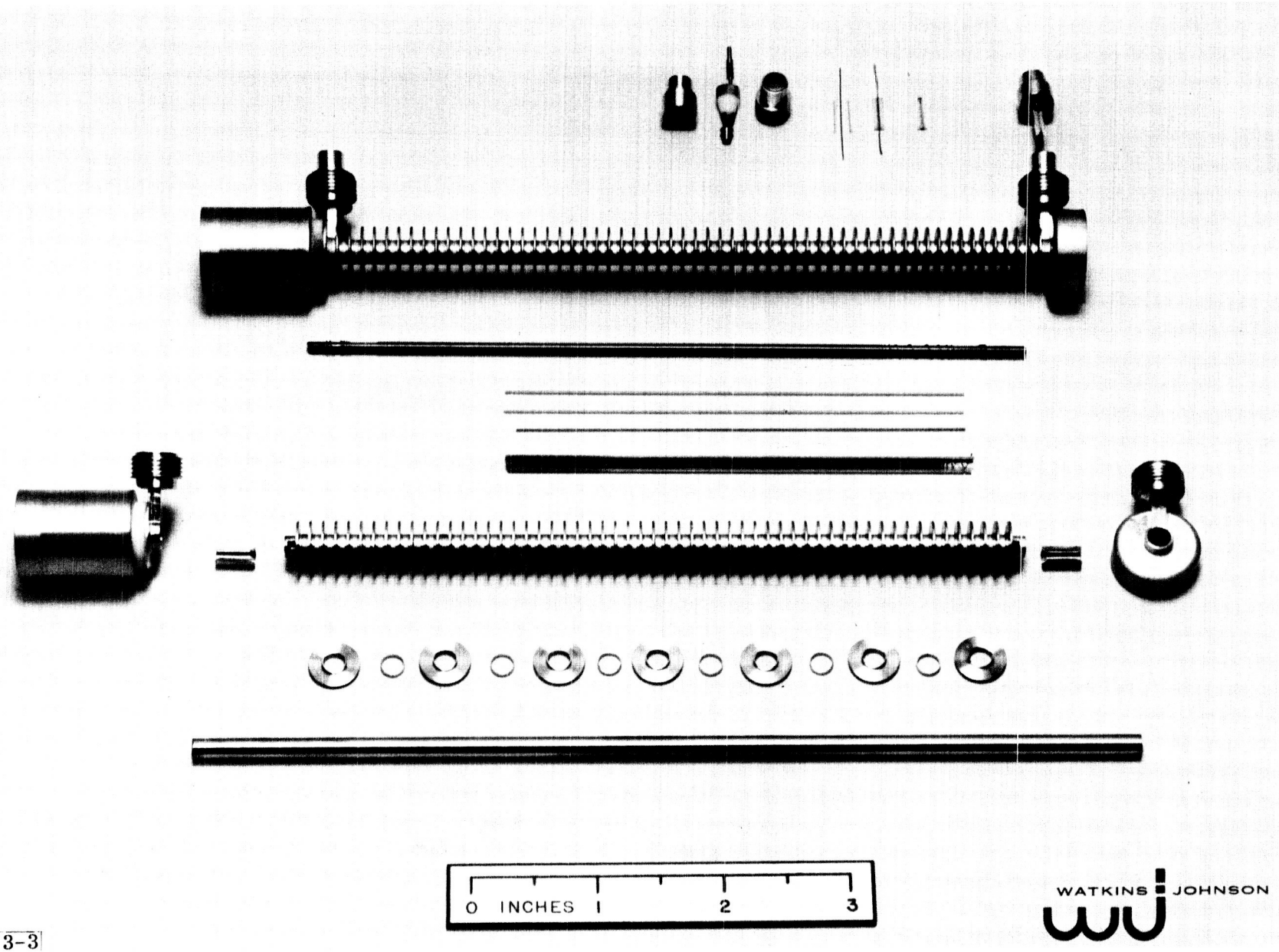

3173-3

Fig. 28 - Photograph showing the WJ-274 body sub-assembly and its component parts including strip transmission line and vacuum window. The helix is a glazed structure using three beryllium oxide wedges for dielectric support.

In the upper part of Fig. 28 the vacuum window can be seen. This window was developed for the WJ-251, 2.5 watt X-band amplifier, and hundreds of windows of this type have been built and used at Watkins-Johnson Company. It is an extremely reliable component. The ceramic part gives a minimum electrical discontinuity and is designed to have an approximately 50 ohms characteristic impedance. It can serve as a very wideband vacuum-window component. It is used in tubes which operate all the way from L through X-band.

Electron Gun Assembly

Figure 29 is a photograph of the electron gun and input transmission line subassembly and their component parts. The parts which make up the header assembly are shown at the left (bottom row). The cathode and focus electrode subassembly and parts are in the center. The white ceramic ring centers and positions the cathode subassembly in the anode. The anode can is made of magnetic alloy so that it not only performs the function of the anode but also serves as its own magnetic shield. The parts of the anode subassembly are shown in the upper row. The metallized ceramic ring, which is seen in edge view in the finished assembly, serves as insulator between the anode and the body (helix) potential. This allows the anode to be operated above helix potential to block ions from reaching the cathode. This scheme of designing the electron gun so that the anode can also serve as the magnetic shield provides the smallest diameter shielded electron gun assembly that can be easily built. The outer diameter of this can is determined by the required radial dimensions of the insulating ceramic (set by allowable voltage gradient) and the diameter of the focus electrode (which is set by cathode diameter).

Collector Assembly

Figure 30 is a photograph of the collector subassembly showing the relationship of its parts. This is a complete two stage collector. The metallized ceramic insulator closest to the pumping tubulation serves the double purpose of providing the electrical insulation between collector stages and also the insulation and heat conduction path between the stages and ground.

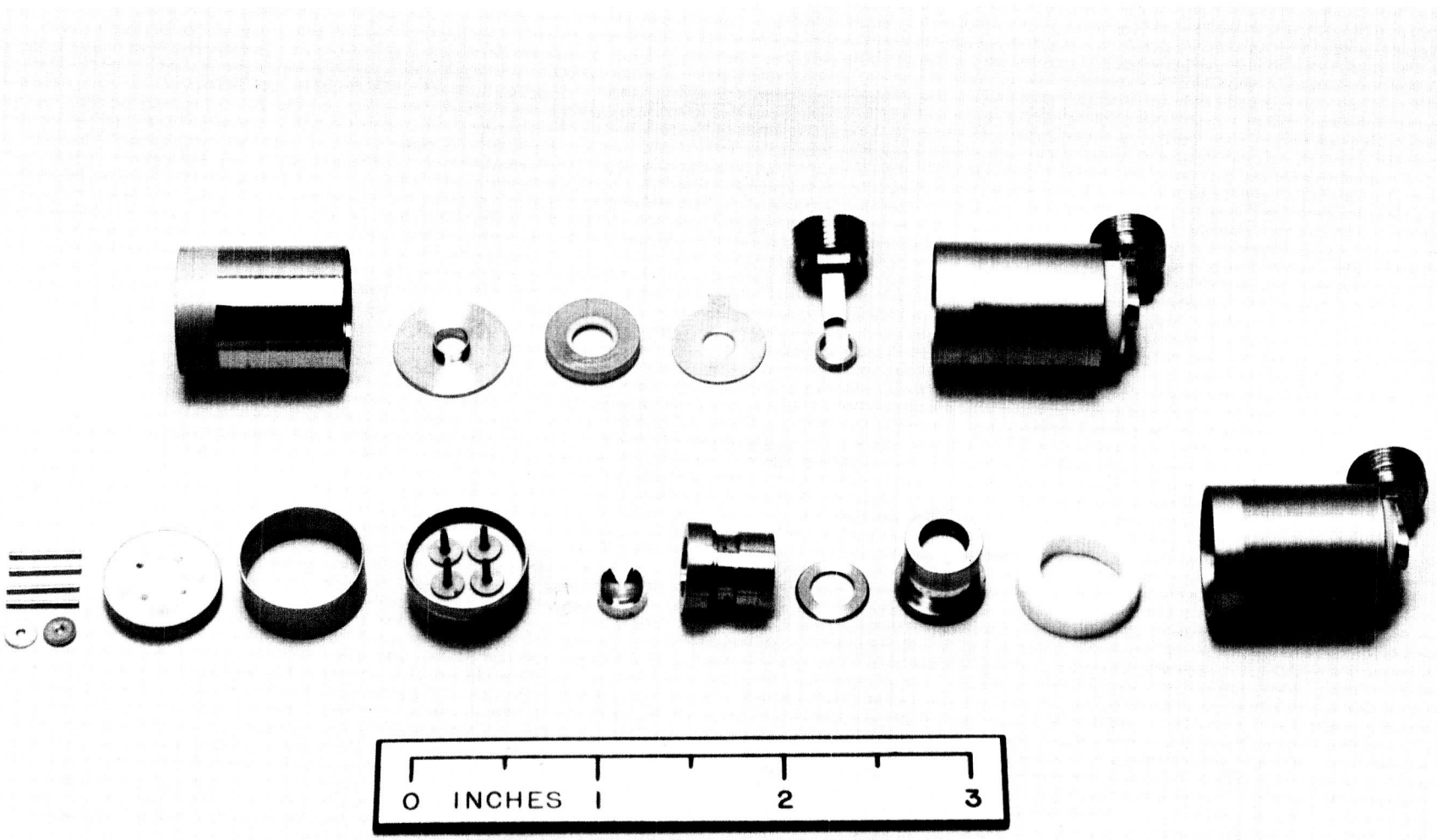

WATKINS JOHNSON

3173

Fig. 29 - Photograph of the electron gun and input stripline subassembly and component parts. The lower row shows the header components (at left), the cathode subassembly, cathode insulating ceramic and anode subassembly. The upper row shows the parts which make up the anode subassembly.

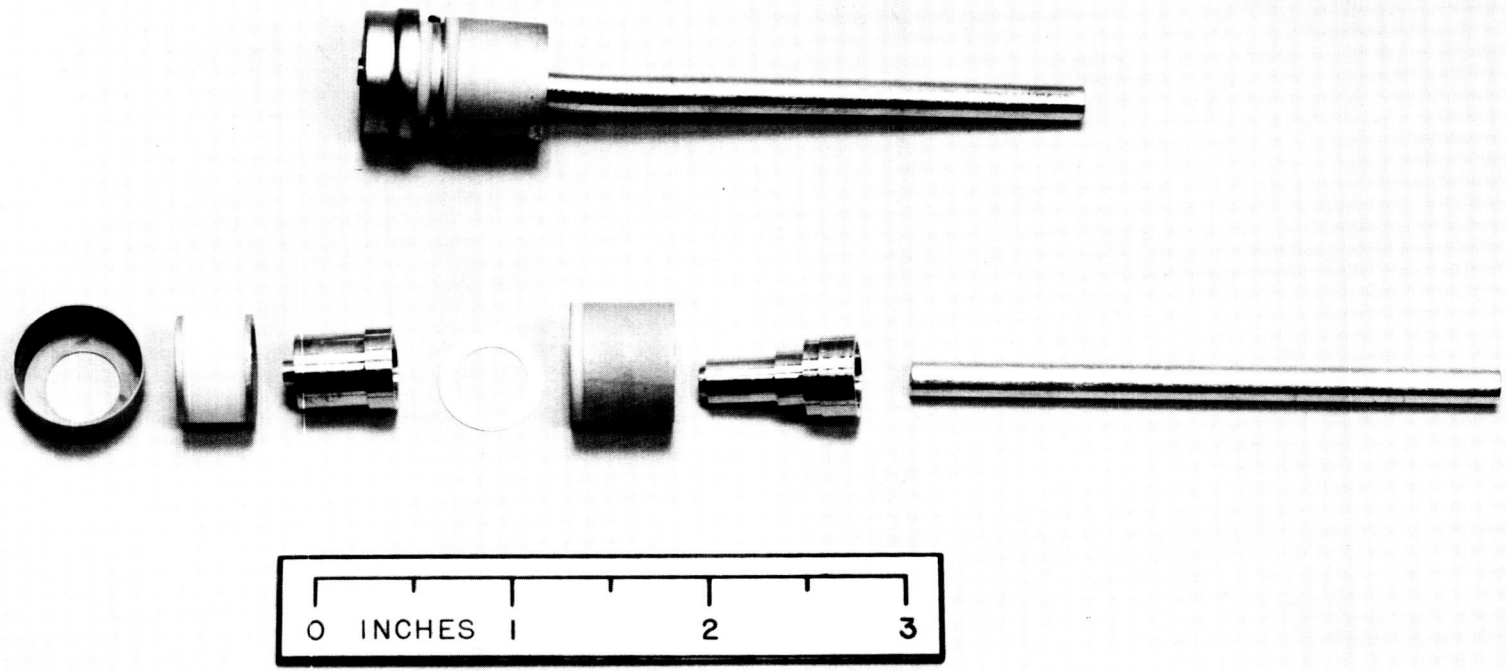

WATKINS JOHNSON

3173-2

Fig. 30 - Photograph of the collector subassembly and its component parts. This is a complete two stage collector assembly including the metallized ceramic insulator which serves to insulate and also conduct heat from the two stages to the capsule.

Encapsulation

The tube is mounted in a rectangular capsule shown in Fig. 31. Heat is drained from the collector, gun and body by thermal conduction through the capsule where it is transferred to the heat sink through the bottom surface. Insulation of the high voltage flying leads is accomplished by potting materials which properly insulate and support the high voltage elements and terminals from the capsule which is at ground potential. This encapsulation and mounting method performs its function of support and cooling and has been tested over a wide range of environmental conditions which include random vibration (20 g rms random, 5 - 2000 Hz), temperature (soak, turn-on, and operation in the range of -50° C to $+100^{\circ}$ C), mechanical shock (60 g, 11ms and 110 g, 8 ms), static acceleration (100 g), vacuum (sea level to space vacuum through critical pressure) and thermal shock (-50° C to $+100^{\circ}$ C in 5 mins.). The total weight of the unit shown in Fig. 31 is 15.9 ounces.

Figure 32 shows a photograph of a lighter weight version of the capsule which can meet an overall weight specification of 12 ounces.

Figure 33 shows another version of the capsule which has mounting feet providing mounting access from above. This is necessary in certain low access, tight packing requirements. This version also uses light weight, low profile OSM connectors.

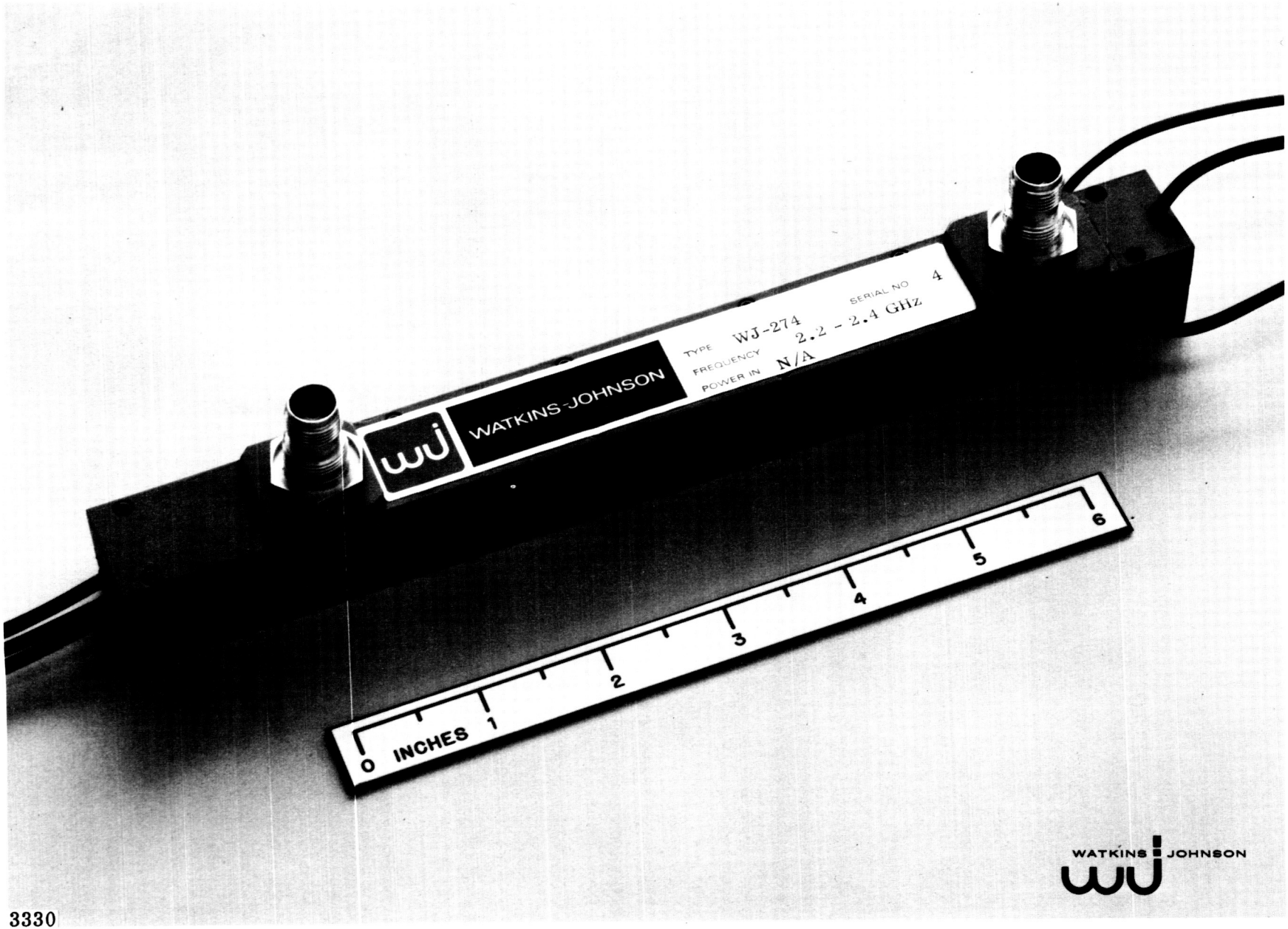

Fig. 31 - Photograph of the encapsulated WJ-274 No. 4.

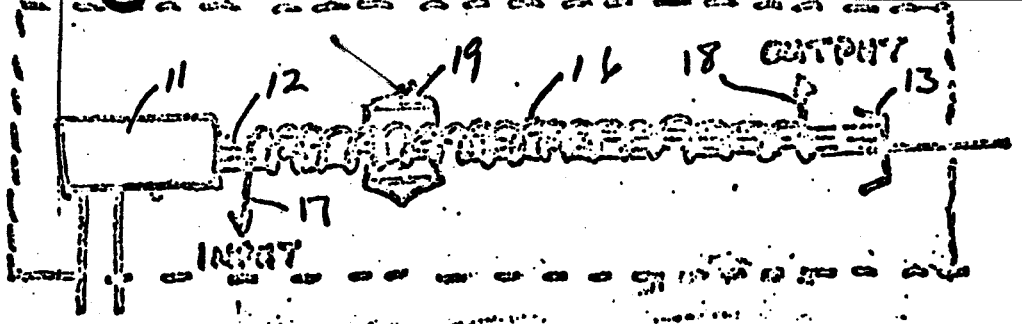

Figure 1

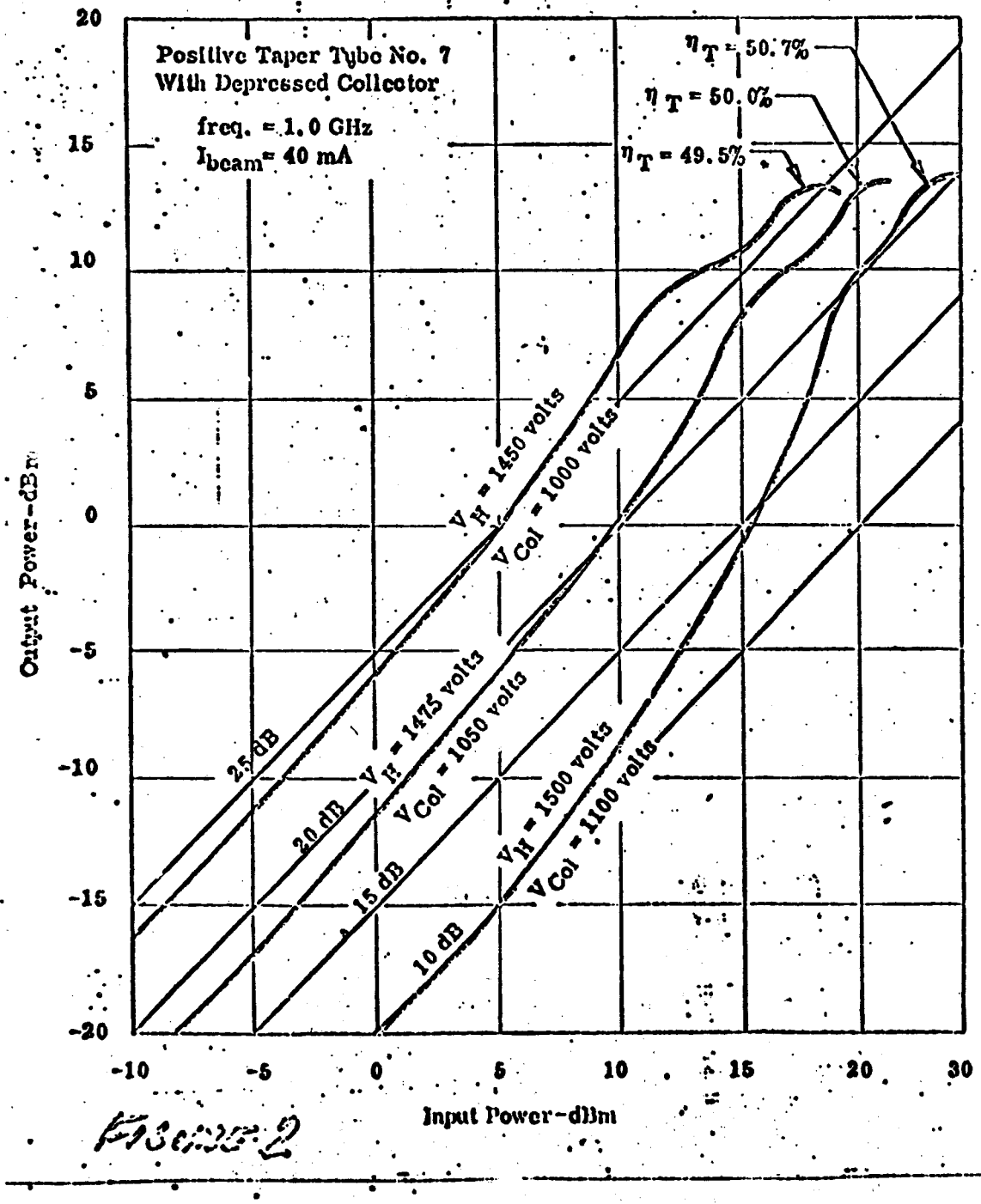

Figure 2

APPENDIX I

DETAILED SPECIFICATIONS AND ACHIEVED PERFORMANCE

NAS1 - 3766 Exhibit A	Achieved Performance
Electrical Characteristics	
Frequency Range:	
2,200 to 2,300 MHz	2,100 to 2,500 MHz
Nominal Operating Frequency Band:	
2,290 to 2,300 MHz	2,290 to 2,300 MHz
Saturated Power Output:	
Shall be 20 watts, ± 1 watt, within the nominal operating frequency band; shall be capable of adjustment to a saturated power output of 20 watts, ± 1 watt, over any 10 MHz band within the overall frequency range.	20 watts. Tube can be operated over the range of 10 to 50 watts.
Bandwidth:	
The saturated power output variation over any ± 5 MHz band, within the specified frequency range, shall be 0.2 dB (or less) for a constant input signal.	Meets specification.
RF Input:	
Shall not exceed 20 milliwatts for a saturated power output of 20 watts, ± 1 watt.	Various experimental tubes had different requirements. Capability was shown of producing 20 watts with 8 milliwatts input.
Spurious Coherent Output:	
Shall be 50 dB (or greater) below the primary coherent output.	At least 75 dB below carrier.

APPENDIX I
(Continued)

DETAILED SPECIFICATIONS AND ACHIEVED PERFORMANCE

NASA - 3766 Exhibit A	Achieved Performance
Electrical Characteristics	
Second Harmonic Output:	
Shall be 15 dB (or greater) below the fundamental output.	23 dB below carrier
Noise Figure:	
30 dB, maximum	Showed that 23 dB noise figure could be achieved with proper design. Experimental tubes gave between 30 and 40 dB at full power and efficiency.
Input Impedance:	
50 ohms, ± 10 percent, with a maximum VSWR of 1.5:1, while tube is operating.	Meets specification. VSWR <1.2
Output Impedance:	
50 ohms, ± 10 percent, with a maximum VSWR of 1.5:1, while tube is operating.	Operating VSWR not measured. Probably much higher. VSWR (non-operating)<1.2
Load Stability:	
There shall be no evidence of spurious oscillation occurring in the tube when a load with a VSWR of 1.5:1 is cycled through a line length of one-half wavelength.	Meets specification.
Phase Linearity:	
The output phase shall not vary more than 3.0 degrees over any 10 MHz frequency band, within the specified frequency range.	Meets specification.

APPENDIX I
(Continued)

DETAILED SPECIFICATIONS AND ACHIEVED PERFORMANCE

NAS1 - 3766 Exhibit A	Achieved Performance
Electrical Characteristics	
AM to PM Conversion:	
At saturated power output, the AM to PM conversion shall be 3 degrees (or less) per dB change in input power.	Exceeds specification. Measures 14.5 °/dB at 21 watts out and 35.5 percent efficiency.
Phase Sensitivity:	
The output phase shall not change more than 2 degrees per volt change in helix voltage.	Measures 2.2 °/volt.
Collector Operation:	
A multiple depressed collector design may be employed	Both single and double stage collector tested.
Focusing:	
Cobalt-Platinum Periodic Magnetic focusing may be employed.	Cobalt-Platinum used.
Overall Efficiency (including heater power):	
The overall efficiency for a 20 watt saturated power output shall be 40 percent, or greater.	At 20 watts, 36.6 percent to 37.6 percent achieved across band 2.2 to 2.3 GHz. At 35 watts, 39.3 percent to 40.2 percent achieved across band 2.2 to 2.3 GHz.
Life and Reliability Characteristics	
Beam Transmission:	
Shall be a minimum of 98 percent under normal operating conditions. Normal operating conditions are defined as any operation which is within the limits of paragraphs 2.1.2.4.	At 20 watts and 37 percent efficiency, beam transmission equals 92.5 percent.

APPENDIX I
(Continued)

DETAILED SPECIFICATIONS AND ACHIEVED PERFORMANCE

NAS1 - 3766 Exhibit A	Achieved Performance
Life and Reliability Characteristics	
Helix Interception:	
The helix must be capable of 10 percent helix interception over the helix length without physical damage to the helix or excessive shortening of cathode life.	Capable of intercepting in excess 40 percent of beam current on helix at saturated output level of 20 watts without damage.
Cathode Life:	
50,000 hours, design minimum.	Designed to specification requirements.
Cathode Type:	
Oxide coated.	Oxide coated.
Mechanical Characteristics	
Length:	
Shall not exceed 7.0 inches, excluding connectors or leads. Minimum length shall be a design objective.	8.75 inches.
Volume:	
Shall not exceed 16 cubic inches, excluding connectors. Minimum volume shall be a design objective.	7.1 in^3 (0.9" x 0.9" x 8.75")
Weight:	
Shall not exceed 12 ounces. Minimum weight shall be a design objective.	12 ounces with lightweight capsule. 16.0 ounces with rectangular capsule.

APPENDIX I
(Continued)

DETAILED SPECIFICATIONS AND ACHIEVED PERFORMANCE

NAS1 - 3766 Exhibit A	Achieved Performance
Mechanical Characteristics	
Mounting:	
Mounting provisions shall be consistent with the thermal conduction and other tube design and operating requirements.	Mounted by bolting bottom surface to heat sink.
Cooling:	
Shall be capable of operation by conduction cooling only without any convective augmentation.	Conduction cooling through bottom surface.
DC Power Connections:	
Flying leads.	Flying leads.
RF Input Connector:	
Type TNC or TM; TNC preferred.	TNC or OSM.
RF Output Connector:	
Type TNC or TM; TNC preferred.	TNC or OSM.
Type of Construction:	
Metal-Ceramic.	Metal-Ceramic.
Environmental Characteristics	
The TWT shall be capable of operating before, during and after subjection to any environmental conditions, or combination of environmental conditions, specified below:	
Static Acceleration:	
50 g in each direction, along each of three (3) mutually perpendicular axes.	100 g, 3 axes.

APPENDIX I
(Continued)

DETAILED SPECIFICATIONS AND ACHIEVED PERFORMANCE

NAS1 - 3766 Exhibit A	Achieved Performance
Environmental Characteristics	
Vibration:	
2.1.2.4.2.1 Sinusoidal: Sweep at rate of 2 minutes/octave, along each of three (3) mutually perpendicular axes: 0.5" D. A., 5 cps to 18 cps ± 25 g (vector) 18 cps to 2,000 cps	High level sinusoidal not tested.
2.1.2.4.2.2 Random (Gaussian band limited):	
12 minutes along each of the three (3) mutually perpendicular axes: 0.10 g^2/cps, 20 - 2,000 cps.	5 minutes each of 3 planes 20 - 59 cps at 0.04 g^2/cps 59-126 cps at 9 dB/octave 126-700 cps at 0.40 g^2/cps 700-900 cps at minus 18 dB/octave 900-2000 cps at 0.09 g^2/cps
Shock Acceleration:	
70 g, 11 milliseconds, each axis, each direction.	60 g, 11 ms, 8 shocks each of 3 planes 110 g, 8 ms, tube axis.
Pressure:	
760 mm t0 10^{-8} mm of Hg.	760 mm to 10^{-5} mm of Hg (tested)
Humidity:	
90 percent	90 percent relative humidity.
Temperature:	
Continuous operation at any heat sink temperature within the range -40° C to +85° C.	Continuous operation at any heat sink temperature from -50° C to +100° C.

APPENDIX II

TABULATION OF TYPICAL WJ-274 DESIGN PARAMETERS

f_o	2.3 GHz
v/c	0.059
TPI	60
γa	0.95
2a	0.091 in.
Helix loss/wavelength	.15 dB/λg
b/a	0.6
Magnet period, L	0.206 in.
r_1/L (Sterrett-Heffner)[7]	0.432
R_2/R_1 (Sterrett-Heffner)[7]	2.11
d_1/L (Sterrett-Heffner)[7]	0.204
B_{pk}, Peak magnetic field	1050 gauss
V_o	1630 V
I_o	50 mA
Beam perveance	0.8×10^{-6} pervs.
J_o, Beam current density	3.3 amps/cm^2
C	.114
QC	.256
$\lambda p/L$	4.85
$\lambda s/L$	2.0

APPENDIX II
(Continued)

VARIATIONS IN DESIGN FROM TUBE TO TUBE

Tube No.	Helix TPI		Active Helix Length		Magnet Period
	Input	Output	Input	Output	
1	58	58	1.3"	2.67"	.206"
2	58	58	1.3"	2.67"	.206" except .186 last 12 cells
3	60	60	1.3"	2.67"	.206" except .160 last 14 cells
4	60	60	1.3"	2.67"	.206"
5	58	58 → 66 (last 0.79")	1.3"	2.67"	.206"
6	63.5	63.5	1.3"	2.73"	.206"
7	67.5	67.5	2.32"	2.73"	.206"
8	58	67.5	1.30"	2.73"	.206"
9	58	67.5	1.30"	3.73"	.206"

BIBLIOGRAPHY

1. Scott, Allan W.: Why a Circuit Sever Affects Traveling-Wave Tube Efficiency. IRE Trans. on Electron Devices, vol. ED-9, no. 1, Jan. 1962 pp. 35-40.

2. Cutler, C. C.: The Nature of Power Saturation in Traveling-Wave Tubes. BSTJ, vol. 35, Nov. 1956, pp. 1285-1346.

3. Tien, P. K.: Walker, L. R.: and Wolontis, V. M.: A Large Signal Theory of Traveling-Wave Amplifiers. Proc. IRE., vol. 43, Mar. 1955, pp 260-277.

4. Rowe, J. E.: A Large Signal Analysis of the Traveling-Wave Amplifier. Technical Report No. 19, Electron Tube Laboratory, University of Michigan.

5. Pierce, J. R.: Traveling-Wave Tubes. D. Van Nostrand Co. 1950.

6. Brewer, George R.: Birdsall, Charles K.: Normalized Propagation Constants for a Traveling-Wave Tube for Finite Values of C. Technical Memorandum No. 331, Electron Tube Laboratory, Hughes Aircraft Company, Oct. 1953.

7. Sterrett, J. E.: Heffner, H.: The Design of Periodic Magnetic Focusing Structures. IRE Trans. of Electron Devices, vol. ED-5, no. 1, Jan. 1958 pp. 35-42.